ADVANCED SENSOR RESEARCH Open Access
www.advsensorres.com

Advances in Electrochemical Urea Biosensors: Trends and Future Prospects

Samar Shurbaji, Arshad Khan, Mohammad K. Hassan, Amine Bermak, Wen-Di Li, Kabir H Biswas, and Bo Wang**

Urea, a nitrogenous organic compound resulting from protein metabolism, is excreted as a waste product in urine. Elevated blood urea levels are associated with severe health conditions, including chronic kidney disease (CKD) and liver failure. Thus, monitoring urea levels is essential for CKD patients and individuals with metabolic disorders that heighten the risk of CKD. While existing diagnostic technologies offer high sensitivity and specificity, they are often expensive, require skilled operators, involve lengthy processing times, and are typically invasive and discontinuous. To address these challenges, researchers have developed various biosensor systems for rapid and cost-effective urea detection. This review provides a comprehensive overview of recent advancements in urea biosensing technologies, highlighting key challenges and potential solutions in biosensor design. It examines enzymatic and non-enzymatic urea biosensors, focusing on electrochemical detection techniques such as amperometry and potentiometry for enzymatic sensors and cyclic voltammetry for non-enzymatic sensors. Additionally, it explores material innovations, technological advancements, and strategies to enhance sensitivity, selectivity, portability, and stability. The integration of biosensors with IoT for real-time monitoring and their applications in medical diagnostics are also discussed.

1. Introduction

Urea (*carbamide*) is a nitrogenous organic compound with the chemical formula $CO(NH_2)_2$.[1,2] It is produced in the liver as a byproduct of the digestion of dietary proteins and expelled as a waste product in the urine to get rid of extra nitrogen. Urea is present in various body fluids, including urine, blood, tear, and sweat.[3] It can pass through the cell membrane and into the blood and tissues due to it's water solubility. The highest concentration of urea exists in urine because the majority of it is eliminated as waste after being filtered by the kidney. In general, urea can be detected as either the entire compound or only its nitrogen component (blood urea nitrogen, or BUN); the reference range for urea nitrogen is 5 – 20 mg dl^{-1}. While urine urea level is affected by the amount of protein consumed, consumption of recommended amounts of protein does not result in elevated urine urea levels.[4,5] Since the kidneys remove 85% of urea, excessive blood urea levels are a sign of kidney dysfunction (owing to decreased renal clearance); elevated blood urea is known as uremia, or blood urine. This disorder occurs in chronic kidney disease (CKD) and can result in end-stage renal failure.[6,7] On the other hand, a diet heavy in protein might cause elevated urea levels in the urine, which is linked to bladder cancer.[8] **Figure 1** illustrates the fate of urea in human body including its production and excretion.

CKD is a critical global health concern with ≈10% of the global adult population affected by the disease, according to recent studies.[10,11] Additionally, CKD ranks as the ninth leading cause of death in the United States with about 14% of the population af-

S. Shurbaji, A. Khan, A. Bermak, B. Wang
College of Science and Engineering
Hamad Bin Khalifa University
Doha 34110, Qatar
E-mail: arkhan4@hbku.edu.qa; bwang@hbku.edu.qa

The ORCID identification number(s) for the author(s) of this article can be found under https://doi.org/10.1002/adsr.202500117

DOI: 10.1002/adsr.202500117

S. Shurbaji
College of Dental Medicine
QU Health, Qatar University
Doha 2713, Qatar

M. K. Hassan
Center for Advanced Materials
Qatar University
Doha, Qatar

W.-D. Li
Department of Mechanical Engineering
University of Hong Kong
Hong Kong, China

K. H Biswas
College of Health and Life Sciences
Hamad Bin Khalifa University
Doha 34110, Qatar

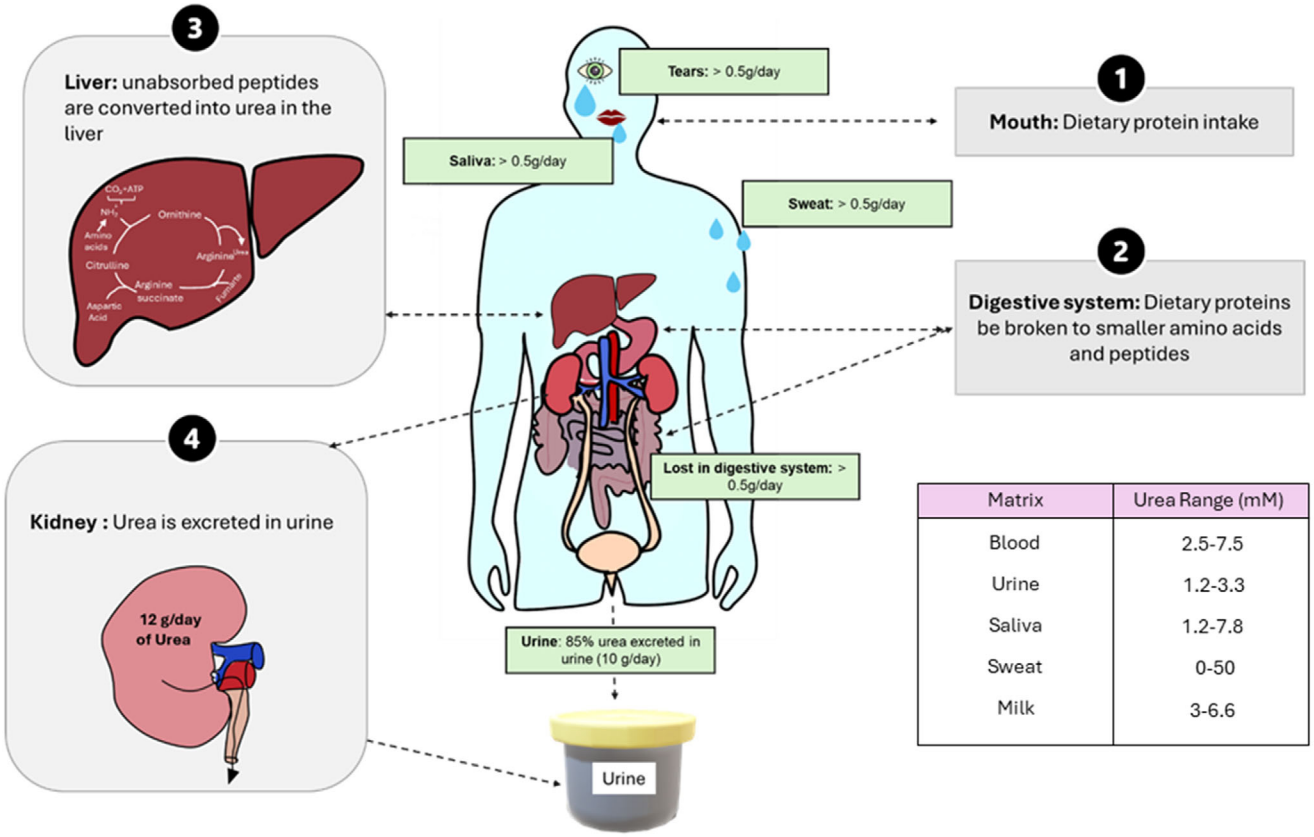

Figure 1. Urea Metabolism and Excretion in the Human Body: This figure illustrates the metabolic pathway of urea in the human body. Dietary proteins are broken down into amino acids and peptides, which are then converted into urea in the liver through the urea cycle. The majority of urea is produced in the liver and excreted through urine. Once synthesized, urea is distributed in body fluids, with a small fraction released through sweat (particularly during exercise), as well as in tears and saliva. The table is reproduced with permission.[9] Copyright 2023, Elsevier.

fected by the disease [https://www.cdc.gov/kidney-disease/php/data-research/index.html].[12] Patients with CKD frequently exhibit elevated serum urea levels. While urea itself was not initially considered toxic at high concentrations in the blood, emerging research indicates that it can cause both direct and indirect toxicity.[13] Specifically, urea can contribute to the development of cardiovascular diseases, significantly increasing CKD-related morbidity. CKD often arises from underlying conditions such as type II diabetes and hypertension, which are highly prevalent worldwide. The International Diabetes Federation reported in 2021 that 10.5% of adults globally have type II diabetes,[14] with 1 in 3 diabetic patients developing CKD, as noted by the US Centers for Disease Control and Prevention (CDC).[12] Moreover, the National Institute of Health (NIH) identified high blood pressure as the second leading cause of kidney disease in the United States, following diabetes.[15] For this, urea detection and monitoring are necessary, particularly for people with different metabolic disorders, to mitigate the risk of kidney or liver diseases and to manage the toxic effects of high blood urea concentrations.[16] Patients with high urea levels may experience various symptoms, including intellectual disability, fatigue, shortness of breath, nausea, vomiting, and unexplained weight loss.[17,18] If untreated, symptoms may get worse, such as the appearance of yellow or white crystals in the skin due to urea excretion through sweat and a urine-like odor on the breath. Prolonged high urea levels can result in significant complications, such as anemia, hypertension, acidosis, thyroid dysfunction, and infertility.[19] Conversely, abnormally low urea concentrations may indicate liver failure or cirrhosis.[20] Both, high or low urea levels can also stem from factors beyond renal or hepatic failure. For instance, dehydration, starvation, infection, and certain medications that can elevate urea levels, whereas overhydration and pregnancy can lead to reduced levels.[21]

Various analytical techniques have been developed for the detection and quantification of urea, including solid-phase extraction chromatography,[22] chemiluminescence-based methods,[23] colorimetric assays,[24] spectrophotometry,[25] mass spectrometry,[26] fluorimetry,[27] and electrochemical detection.[9] However, many of these conventional methods are limited due to their inherent drawbacks. For instance, they often involve complex sample pre-processing, which extends the analysis and detection time. Additionally, these methods typically require highly trained personnel, increasing both the effort and associated costs. Furthermore, urea testing also demands sophisticated and expensive equipment, necessitating a substantial budget. While colorimetric techniques offer simplicity and potential, they usually require additional tools such as scanners, cameras, or phone cameras integrated with computer programs for color analysis or

other advanced instruments to measure color intensities.[28] Finally, most conventional urea tests rely on blood samples, and the phlebotomy process can be inconvenient for both patients and medical staff.[2,29] Moreover, for patients with impaired kidney function, continuous monitoring of urea level fluctuations is more beneficial than relying on isolated measurements.[30]

Significant advancements have been made in urea detection, aiming to address the limitations of conventional methods, particularly through the development of urea biosensors based on various biochemical and biophysical phenomena.[31,32] The first urea biosensor developed in 1969[32] relied on changes in pH to detect urea levels. This process relies on the enzyme urease, which catalyzes the hydrolysis of urea into ammonium and bicarbonate ions. These ions alter the pH of the sample, with the concentration of ammonium ions directly correlating to the urea content. While urease-based biosensors are common, their high cost and limited stability have prompted researchers to explore non-enzymatic alternatives. For instance, metal oxides have been employed due to their excellent catalytic activity, stability, and sensitivity, providing a cost-effective solution to the limitation posed by the use of urease. Urea biosensors are classified based on bioreceptor type, transducer mechanism, and the physicochemical reactions employed. Different researchers propose varying categorizations. Singh et al. divided urea biosensors into ten categories, focusing on the types of transistors and materials used, such as graphene, polymers, nanocomposites, and nanoparticles.[33] In contrast, Pundir et al. organized them into two major categories: transducer-based biosensors, further subdivided into six types, and matrix-based biosensors utilizing polymeric materials.[3] Researchers have also explored correlations between blood urea levels and those in other body fluids, such as urine and saliva, offering more accessible and less invasive testing options compared to blood sampling.[34] Among the various fabrication approaches for urea biosensors, the electrochemical method has been widely studied for its potential to enhance detection.[3] This approach includes potentiometric, conductometric, and amperometric methods, which detect ammonium or bicarbonate ions released during urease-catalyzed urea hydrolysis. Electrochemical methods are particularly promising due to their high sensitivity, specificity, and rapid response times, and they have been extensively researched.[9] Furthermore, non-enzymatic electrochemical approaches are being developed, offering an alternative to enzyme-based detection systems.

Significant progress has been made in electrochemical urea detection in recent years, with notable reviews published on this topic. For instance, two comprehensive reviews,[35,36] covered advancements up to 2021, while a 2022 review focused exclusively on the electrochemical potentiometric approach.[37] More recently, Quadrini et al. (2023) presented a concise mini-review offering a limited set of perspectives.[9] In 2024, Mashhadban-K et al. presented a detailed review; however, their focus was restricted to the enzymatic approach.[38] Additionally, several reviews have explored urea biosensors for applications beyond the biomedical domain.[39–41]

This review explores various electrochemical approaches for urea biosensing, encompassing both enzymatic and non-enzymatic methodologies. For enzymatic biosensors, the focus is on electrochemical techniques, particularly amperometry and potentiometry. In contrast, non-enzymatic biosensors are examined through cyclic voltammetric techniques, with an emphasis on material modifications to enhance performance. Non-enzymatic approaches offer potential advantages in cost-effectiveness and stability compared to enzyme-based systems. The review also discusses key technological advancements in urea biosensors, highlighting strategies to enhance sensitivity and selectivity for accurate detection in complex biological samples. Additionally, it addresses trends in miniaturization and portability, aiming to facilitate point-of-care diagnostics and continuous monitoring. Another critical aspect explored is improving stability and extending the operational lifespan of urea biosensors, which is essential for reliable long-term monitoring and reducing sensor replacement frequency. Finally, this review examines the diverse applications of advanced urea biosensors in medical diagnostics, including kidney function monitoring, chronic kidney disease management, and other clinical scenarios where precise urea measurement is crucial for patient care. **Figure 2** demonstrates the current breakthroughs in urea biosensor technology including both enzymatic and non-enzymatic methods, highlighting methods to improve sensor performance, device downsizing, and integration for practical biomedical applications. **Table 1** summarizes the market status of urea biosensor, despite advances in urea biosensor production, there are no urea biosensors available for home monitoring.

2. Types of Electrochemical Urea Biosensors

Various types of transducers have been developed for electrochemical urea biosensors, with the most common being potentiometric, amperometric, conductometric, thermal, optical, manometric, and piezoelectric transducers.[3] This section focuses on studies utilizing the enzymatic approach for urea detection, particularly those employing amperometric and potentiometric methods. These methods often rely on electrode modification using a variety of nanomaterials to enhance sensor performance.

2.1. Enzymatic Electrochemical Sensors

2.1.1. Amperometric Approach

The amperometric approach involves measurement of current generated by a redox reaction occurring between two electrodes. Variants of this method include amperometry, chronoamperometry, and double-setup chronoamperometry.[42] In amperometry, redox species in the sensing layer undergo oxidation or reduction on the transducer surface, producing an electric current. The resulting signal is typically represented as current (A) versus urea concentration.[43] **Figure 3a** provides a general overview of how amperometric biosensors function.

To enhance sensitivity and response time, designing biosensors that enable rapid electron transfer between the biological element and the electrode is critical. Amperometric biosensors have evolved significantly, allowing direct electron transfer through enzyme immobilization on the electrode surface.[44,45] However, enzyme immobilization presents challenges, as inappropriate techniques can result in enzyme denaturation or electrode fouling, which impede electron transfer. Appropriate immobilization

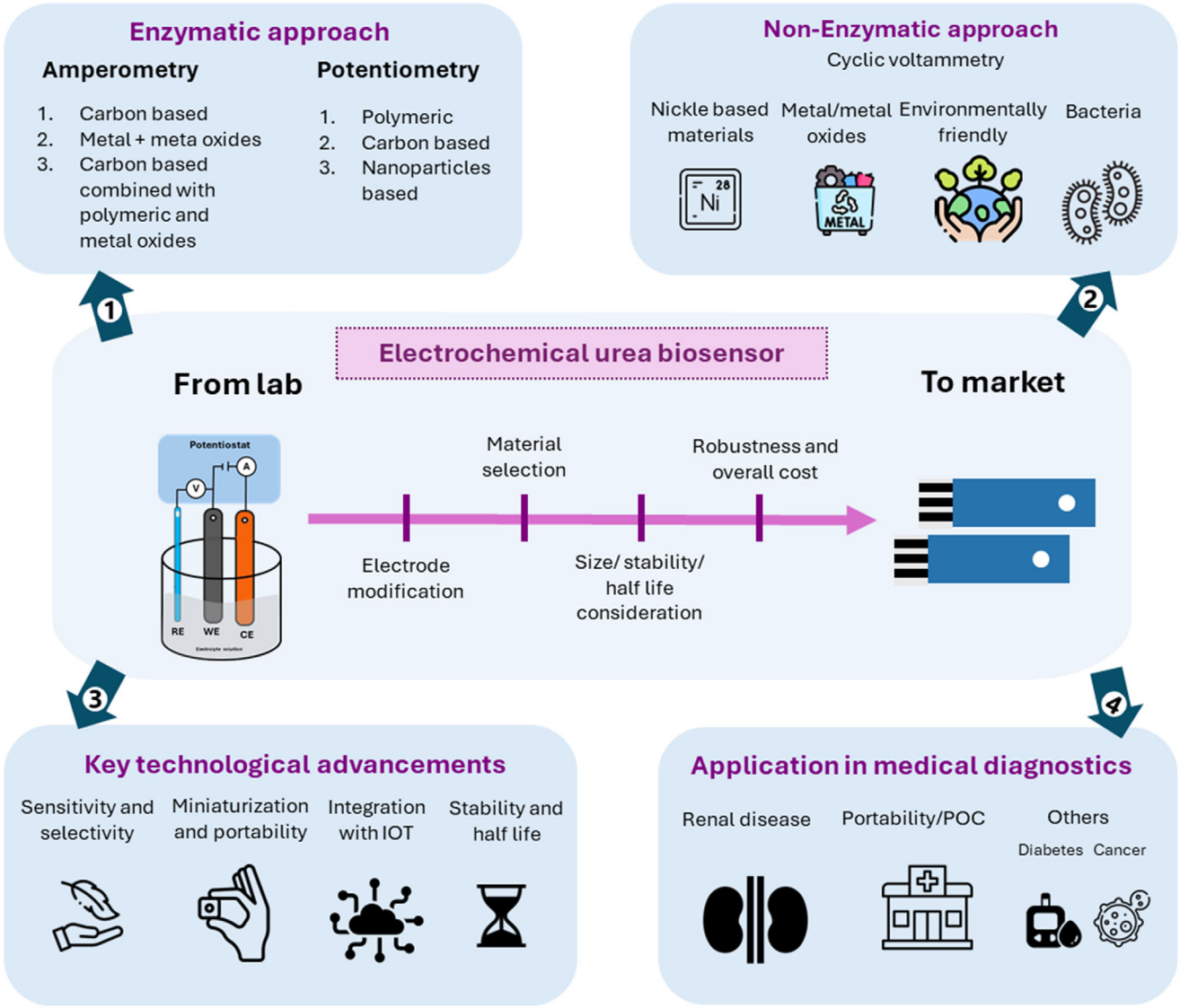

Figure 2. Comprehensive overview of urea biosensor research and development: This schematic provides a detailed overview of advancements in urea biosensor technology, covering both enzymatic and non-enzymatic detection strategies. It illustrates the transition from laboratory research to market-ready applications, highlighting key innovations. Enzymatic biosensors, primarily utilizing urease, are compared with non-enzymatic approaches that leverage novel materials such as metal oxides. The figure also outlines major technological improvements, including strategies to enhance sensitivity, selectivity, and stability, alongside efforts toward miniaturization and IoT integration. Additionally, it showcases various biomedical applications, emphasizing the role of urea biosensors in diagnostics and disease management, particularly for chronic kidney disease and metabolic disorders.

Table 1. Market status of urea biosensor types.

Biosensor type	Research only	Emerging	Marketed (lab/clinic)	Company / product/ re.
Potentiometric (Urease based)			✔	Roche Cobas c 311/501/701/702
	✔			Metrohm DropSens SPEs
Amperometric (urease-based)		✔	✔	Nova Biomedical Stat Profile Prime Plus
	✔			Zimmer & Peacock Urea Sensor
Lab-on-a-chip/Microfluidic	✔	✔		PalmSens SPEs
			✔	Abbott i-STAT Handheld Analyzer
Non-enzymatic (metal oxide)	✔	✔		[9]
Wearable/Continuous Monitoring	✔			Zimmer & Peacock (custom development)

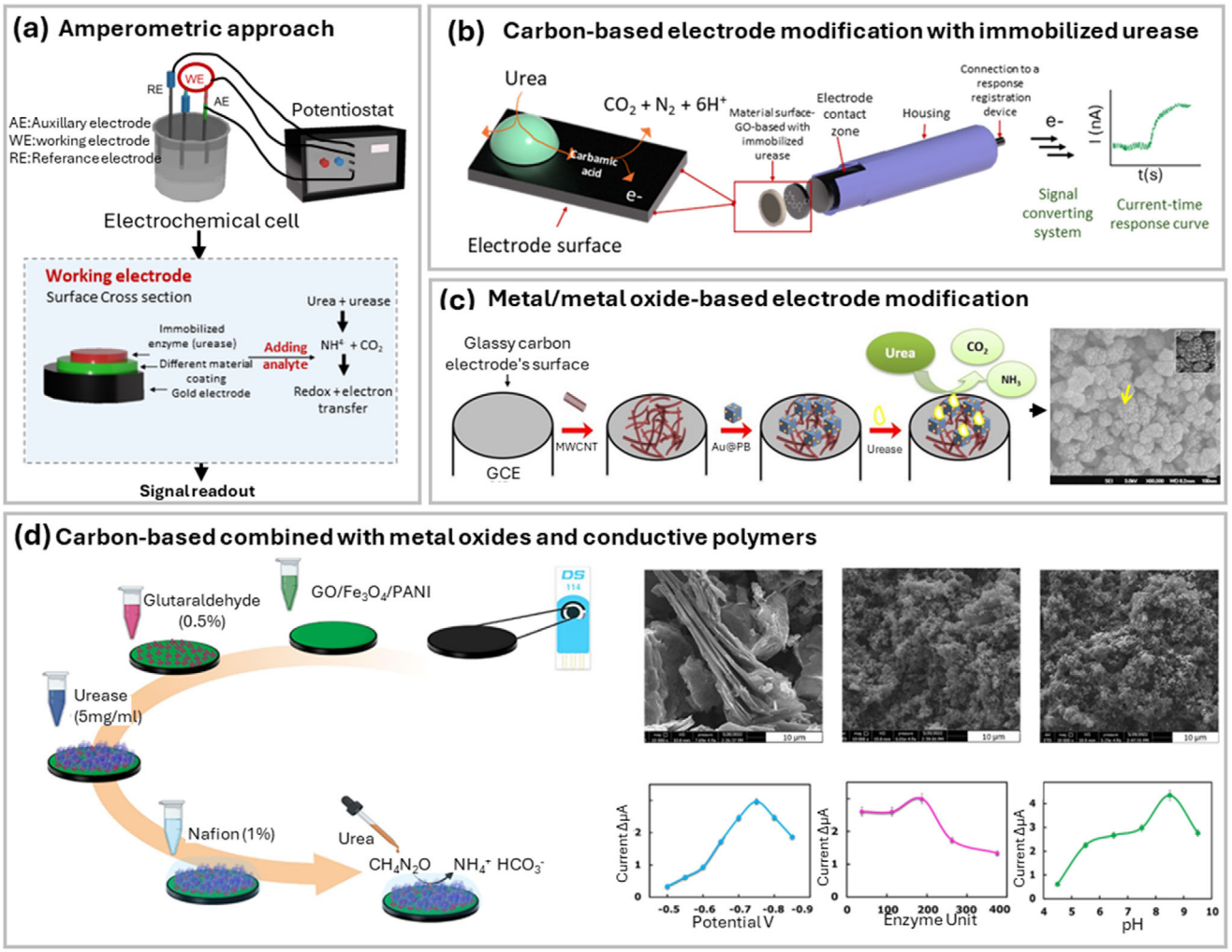

Figure 3. Amperometric Urea Biosensor Mechanisms and Electrode Modifications a) General schematic of an amperometric biosensor. The target analyte (urea) is positioned near the electrode, where enzymatic degradation generates specific products or gases that undergo redox reactions at the electrode surface. When a fixed voltage is applied, electron transfer occurs, generating a measurable current proportional to the urea concentration. A reference electrode provides a stable potential for the working and counter electrodes. Reproduced with permission.[43] Copyright 2011, Elsevier. b) Illustration of a working electrode composed of graphene oxide (GO)-based material with immobilized urease. Urea hydrolysis occurs near the electrode surface, producing carbamic acid, which oxidizes the electrode and generates an anodic current correlated with urea concentration. Reproduced with permission.[50] Copyright 2020, MDPI. c) Schematic representation of a glassy carbon electrode modified with gold nanosphere-decorated Prussian blue nanocubes for enhanced electrochemical performance. Reproduced with permission.[54] Copyright 2023, Springer Nature. d) Preparation steps for a GO/Fe_2O_4-PANI composite as a working electrode, with SEM images of the synthesized composite. The accompanying graphs illustrate biosensor activity in response to varying applied potentials, enzyme concentrations, and pH levels. Reproduced with permission.[61] Copyright 2024, Elsevier.

of urease using suitable matrices is crucial to achieving high sensitivity and reproducibility in these biosensors.[24,32,45]

The amperometric approach is particularly favored for its high selectivity, which eliminates screening thresholds. Current research focuses on improving selectivity and electron transfer through advancements in electrode modifications, enzyme immobilization techniques, or a combination of both. A notable example is the work by Fapyane et al., who developed a novel urea biosensor based on the amperometric approach for CO_2 detection. This biosensor addressed limitations associated with traditional Severinghaus-type CO_2 sensors by modifying both the matrix and the electrode. Their design incorporated a CO_2 microsensor shielded by a gas-permeable membrane, with the urease enzyme immobilized in an alginate polymer matrix using entrapment, stabilization (via stabilizers), and cross-linking agents. The immobilized enzyme layer was placed in front of the CO_2 microsensor within a glass chamber, and the buffer pH was maintained at 6 to favor the production of CO_2 gas during urea hydrolysis. In this system, CO_2 gas diffused through the membrane of the microsensor and was reduced at an Ag cathode. The biosensor demonstrated a linear response to urea concentrations from 0 to 1000 μM, with a low limit of detection (LOD) of 0.94 μM. It achieved a response time of 120 s, which compares favorably with literature values. Additionally, the enzyme retained 70% of its activity after 14 days, highlighting the stability and effectiveness of the biosensor.[46]

Carbon-Based Material-Modified Electrodes: Carbon-based nanomaterials, particularly graphene-based materials, are widely recognized for their exceptional electron transfer properties, stability, and high ion mobility.[47] These characteristics make them highly suitable for electrochemical biosensors. A notable example involves the use of thermally reduced graphene oxide nanoparticles (TRGO) as a response transducer and urease supporter. This approach results in a cost-effective biosensor, as TRGO possesses abundant active groups that facilitate electron transfer and enable electrochemical reactions at low potentials. When combined with urease, TRGO forms a mediator-free biosensor with remarkable sensitivity (2.3 ± 0.1 μA cm^{-2} mM^{-1}), storage stability of up to seven months, and good reproducibility. Figure 3b illustrates the role of graphene oxide-based materials in generating electrochemical oxidation for urea detection.[48] Further advancements have been made using a sonochemical approach to fabricate zinc phthalocyanine/graphene oxide (ZnPh/GO) nanocomposite-modified glassy carbon electrodes. The high density of active sites provided by graphene oxide enhances the catalytic properties of the bioelectrode for urea detection. Moreover, graphene oxide creates a favorable environment for immobilizing urease in high concentrations, facilitating improved electron transfer between the analyte and the ZnPh/GO/Urease bioelectrode surface.[49] Carbon nanotubes (CNTs) and graphene-based materials are also highly recommended for their exceptional electrochemical properties, large surface area-to-volume ratio, electrical conductivity, and stability.[50] For example, Hassan et al. developed a disposable urea biosensor based on a carbon nanotube/poly(o-toluidine) (PoT) nanocomposite. Poly-o-toluidine is known for its high electrochemical signal; however, integrating it with carbon-based materials enhances its electron transfer properties, addressing the reduction in electrochemical activity following urease immobilization. Blood sample analyses using this biosensor exhibited high correlation with reference methods for urea detection.[51] Another innovative application involves using polyacrylonitrile (PAN) nanofibers and multi-walled carbon nanotubes (MWCNTs) to create a composite biosensor for the dual detection of glucose and urea. The nanofiber's large surface area-to-volume ratio and high porosity significantly increase enzyme loading capacity and prolong enzyme lifetime. This biosensor achieved a very low detection limit of 0.1 μM for urea with high accuracy.[52]

Metal and Metal Oxide-Based Electrodes: Metal and metal oxide nanomaterials have been widely explored in urea biosensors due to their superior electrochemical and catalytic properties.

Gold-Based Electrodes: Gold nanoparticles (AuNPs) embedded in polymers have demonstrated significant potential for urea biosensing. Korkut et al. developed a biosensor using gold electrodes coated with poly(propylene-co-imidazole) embedded with AuNPs.[53] Ammonium, a product of enzymatic urea degradation, undergoes electro-oxidation facilitated by the AuNPs in the polymer chain. This sensor exhibited outstanding detection limits, specificity, and storage stability. However, the detection range was not clinically relevant.[42] Prabakaran et al. addressed this limitation by fabricating self-assembled gold nanospheres decorated with Prussian blue nanocubes. Prussian blue acts as a redox mediator, enhancing electron transfer, while gold nanoparticles contribute to electrocatalytic properties. Together, these materials produced a biosensor with excellent performance, including fast response time and high selectivity. Figure 3c illustrates the preparation approach for this modified electrode.[54] In another study, Wang et al. developed a PANI:PSS/AuNPs/SPCE-based sensor for multi-parameter detection of urine components. By combining the high conductivity of PANI with the catalytic activity of AuNPs, the sensor demonstrated enhanced sensitivity and selectivity, making it a promising tool for point-of-care diagnostics.[55]

Platinum-Based Electrodes: Platinum (Pt) is a prominent material recently used for electrochemical studies and the oxidation of different compounds.[32] Uru et al. developed a biosensor using a Poly(pyrrole-co-1-(2-Aminophenyl)pyrrole)/Urease film coated Au electrode, modified with platinum nanoparticles. The sensor achieved a detection limit of 7.58 μM, suitable for detecting blood urea concentrations and other sample types, with an impressive accuracy of 104% (this was calculated by dividing the measure concentration by the actual concentration).[56] Another study by Hosseinian et al. reported immobilizing urease on macroporous polypyrrole (MPPy) and pyrrole on a platinum electrode surface. The polymeric surface increased the urease loading capacity due to its large surface area, while platinum's catalytic properties further enhanced the detection limit. This biosensor demonstrated rapid response times (5–7 s) and high selectivity, making it ideal for clinical applications.[57]

Nickel Oxide-Based Electrodes: Nickel oxide (NiO) is another promising material, valued for its high conductivity, efficient electron and charge transfer, and stability. Tyagi et al. reported a urea biosensor using urease immobilized on NiO. The sensor achieved a sensitivity of 66.7 μA mM^{-1} and a remarkably fast response time of 5 s, highlighting its potential for rapid and reliable urea detection.[58]

Other Electrodes: Some studies have explored the use of alternative metals such as indium and tin. For instance, Mikani et al. developed a highly sensitive biosensor for urea detection in blood serum, utilizing a urease/In_2O_5Sn nano-coated fluorinated SnO_2 platform. This sensor exhibited excellent performance in detecting urea in complex biological samples, highlighting its potential for clinical diagnostics.[59]

Composite Electrodes: The integration of carbon-based materials with metal oxides and conductive polymers has yielded high-performance urea biosensors with enhanced sensitivity and stability.

Graphene-Metal Oxide-Polymer Composites: One study developed a sandwiched electrode structure comprising Indium Tin Oxide (ITO), Polydiphenylamine (PDPA), phosphotungstic acid (PTA), and graphene (Gra). The composite was prepared using an electrochemical deposition technique, resulting in outstanding properties. The biosensor exhibited an excellent linear response to urea concentrations ranging from 1 to 13 μM, with a sensitivity of 1.085 μA μM^{-1} and a rapid response time of 5 s. The unique sandwiched morphology contributed significantly to efficient oxidation and urea detection.[60]

Graphene Oxide (GO)-Polymer-Metal Oxide Composites: In another study by Evli et al., GO was combined with polyaniline (PANI) and Fe_3O_4 nanoparticles to exploit their synergistic properties. The resulting biosensor demonstrated a linear detection range for urea concentrations between 0.01 and 10.0 mM and a detection limit of 0.03 mM. The combination of GO's high surface area, PANI's conductivity, and Fe_3O_4's catalytic properties significantly enhanced the performance of the

Table 2. Comparison in analytical characteristics for various enzymatic amperometric urea biosensors.

	ELECTRODE/mATERIAL USED	MATRIX TYPE	IMMOBILIZATION METHODS	LOW DETECTION LIMIT (LOD)/SENSITIVITY	RESPONSE TIME	REUSABILITY/sTORAGE STABILITY	REFERENCES
1	Ag / CO_2 microsensor	Urease / alginate polymer	(urease/BSA/alginate/ glutaraldehyde/Ca2+)	0.94 μM	2 min	70% enzymatic activity after 2 weeks	[46]
2	Pt/ AgACl/urease	TRGO	Urease/albumin Immobilized on polyurethane Particles	20 μM	25 s	65% enzymatic activity after 20 days Stability: 7 months	[48]
3		Polymer/MWCNTs		0.1 μM 350 ± 19 μA/(mM^{2}cm^2)			[50]
4	Au/polymer/ Au NPs,	Polymeric/Au NPs	Physical adsorption	36 μM	-	97% after 75 days	[52]
5	Ag/AgACl /urease	Urease /Au NPs decorated Prussian blue nanocubes and multi-walled carbon nanotubes.	-	0.32 mM	20 s	-	[53]
6	GCE	Urease/ ZnPh/GO	-	34 μM	10 s	94% after 8 weeks	[49]
7	Ag/AgCl	Carbon nanotube/poly(o-toluidine)	Glutaraldehyde	30 μM	-	-	[51]
9	Au electrode	(PtNPs) / Poly(pyrrole-co-1-(2-Aminophenyl)pyrrole)/Urease	Chemical immobilization	7.58 μM 31.8 μA /(mM cm^2)		100% after 14 days & lost 22% after 28 days.	[55]
9	Pt electrode	Polypyrrole and macroporous polypyrrole	Glutaraldehyde	0.208 mM 0.0432 mA mM^{-1}	5 s	96% after being used 6 times. 93% after a month	[32]
10	Bioelectrode	NiO thin film	Physical adsorption	0.28 mM 66.7 μA/(mM)	5 s	2 weeks	[56]
11	Screen Printed Electrode	GO, PANI, and Fe_3O_4		0.03 mM			[58]

biosensor.[61] Another approach involved the development of a composite biosensor incorporating urease enzyme, graphene oxide, gold nanoparticles, and chitosan, all deposited onto a pencil graphite electrode. This biosensor was successfully applied for urea detection in serum samples from both healthy individuals and patients with renal disorders. It exhibited a wide linear range (0.1–1.0 mg mL^{-1}), a low detection limit (0.9956 mg mL^{-1}), and demonstrated satisfactory selectivity, sensitivity (0.00555 μA mg^{-1} mL^{-1} cm^{-2}), and stability.[62] Additionally, a sulfonated polypyrene aniline/polyaniline composite reinforced with Cu-GQD@ZIF8 (copper-graphene quantum dots embedded in ZIF-8) was also reported. This composite material significantly enhanced the electrocatalytic activity and sensitivity of the biosensor, enabling efficient urea detection. The approach demonstrated high sensitivity, selectivity, and stability, making it a promising tool for urea detection in both clinical and environmental applications.[63]

Polymer Composite: Uzunçar et al. reported a study on a polyaniline:polystyrene-sulfonate (nano-PANI:PSS) composite for catalyst-free ammonium (NH_4^+) sensors and enzyme-coupled urea biosensors. The fabricated nanostructured material featured interconnected fibers (≈50 nm in diameter) and exhibited superior electrochemical properties and processability. The urea biosensor demonstrated a linear detection range of 0.2–0.9 mM with a sensitivity of 41 mA cm^{-2} M^{-1}. Additionally, the sensor exhibited high selectivity in a urine model, marking a significant advancement in the development of printed organic sensors and biosensors.[64]

Figure 3d illustrates the preparation process and key outcomes of carbon-based composite biosensors. **Table 2** summarizes the reported studies, highlighting the key materials, methods, and performance metrics.

2.1.2. Potentiometric Approach

Most reported urea biosensors utilize potentiometric transducers, a classical technique that dates back to before the 20th century. This approach measures the potential difference between two electrodes—an ion-selective electrode (ISE) and a reference electrode—without any current flow between them. The voltage measured is directly related to the analyte concentration, with the relationship described by the Nernst equation:

$$E = E_0 \mp \left(\frac{RT}{nF}\right) lna_1 \quad (1)$$

Here E_0 is the standard potential, R is the universal gas constant, T is the absolute temperature in Ko, n is the total number of charges on the ion, F = Faraday constant, and a_1 is the analyte activity.[65] Wang (2006) provides a detailed explanation of how potentiometric sensors operate.[66] In a typical potentiometric urea sensor, urea is hydrolyzed into ammonium and bicarbonate ions by the urease enzyme immobilized on the electrode. The ion-selective electrode detects these ions, and the urea concentration is subsequently calculated.[9,65–68] Potentiometric urea biosensors have been extensively used for decades. However, significant advancements have emerged in recent years, primarily driven by innovations in material science and the incorporation of nanomaterials.[69]

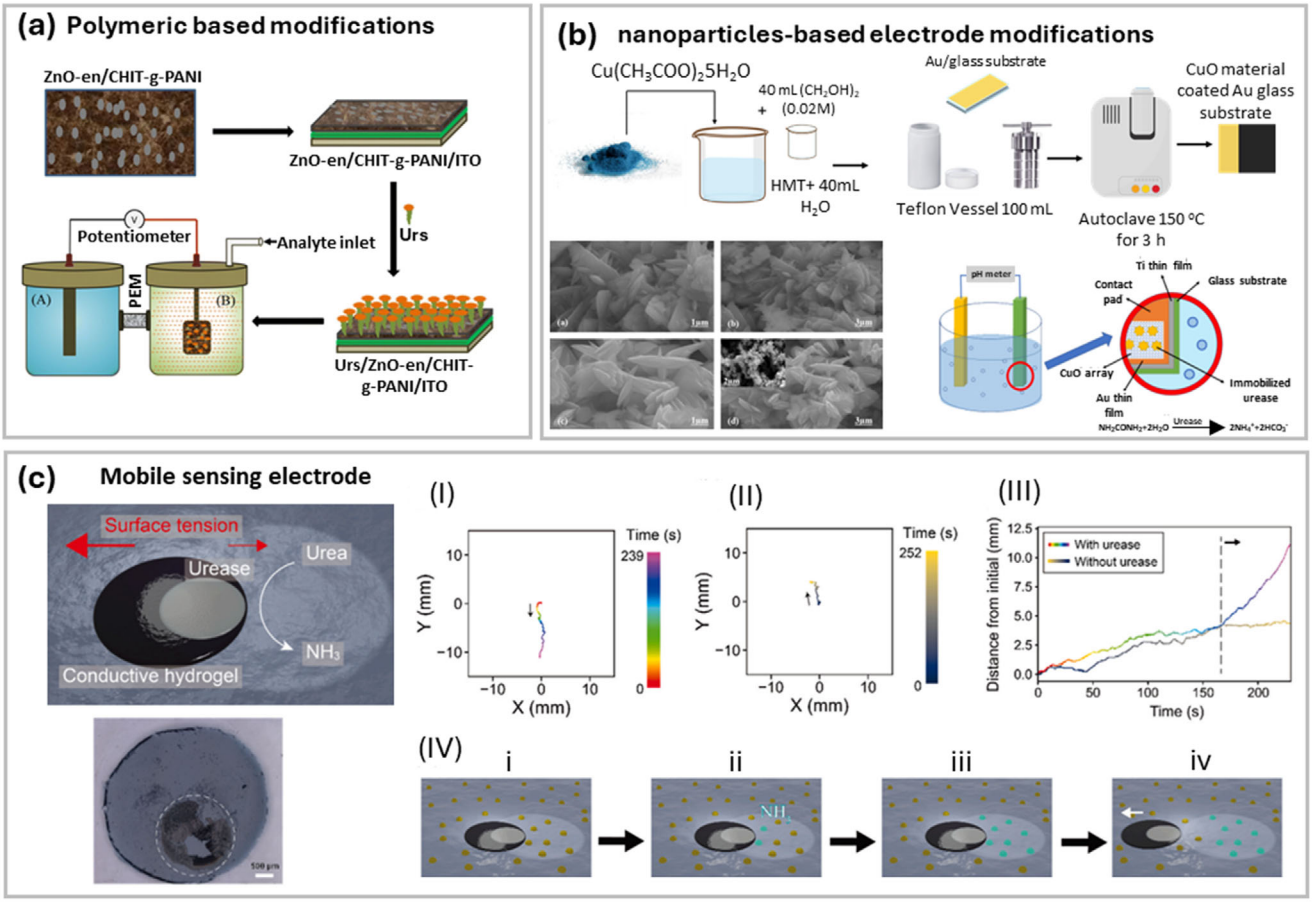

Figure 4. Experimental Design and Motion Analysis of Urease-Based Conductive Hydrogels: a) schematic experimental design of the polymeric-based particles (ZnO/ PANI/ chitosan). Reproduced with permission.[76] Copyright 2020, Springer Nature. b) Hydrothermal synthesis of CuO nanostructured material. It also shows SEM micrograph for CuO and mixed solvent CuO. Along with the urea detection process utilizing urease-functionalized CuO nanostructures with chain-like morphology. Reproduced with permission.[87] Copyright 2024, Elsevier. c) represents the overall principle of urea detection; the dashed circle is showing the hydrogel where urea is immobilized. represents the motion analysis of the conductive hydrogel with urease (I) and without urease (II), a 1 M urea solution with a phosphate buffer (ionic strength of 10 mM and pH 5.7), motion was observed. The rainbow color in panel (I) (ranging from red to purple) and the cividis color in panel (II) (ranging from navy blue to ochre) indicate this motion. The recording was taken from a top view of the buffer solution for ≈4 min (239 s in panel (I) and 252 s in panel (II). (IV) Conductive hydrogels prepared using an 8 µl dispersion of PEDOT: PSS-DMSO, showed motion, with initial positions set as the origin point on 2D graphs, as indicated by black arrows. he distance from the initial hydrogel position is shown at each time point. Rainbow and cividis colors correspond to the hydrogel position in panels (I) and (II). The gray dashed line represents the time ≈170 s. The schematic of urease-induced motion involves placing the urease-modified conductive hydrogel motor at the air/solution interface (i). The conductive hydrogel is depicted as black circles, modified urease as a white layer, and urea molecules as yellow spheres. Urea is then converted to ammonia catalyzed by urease (ii), with ammonia molecules represented by cyan spheres. As time progresses, the amount of ammonia increases (iii), leading to movement of the urease-modified conductive hydrogel in the opposite direction of the ammonia-rich area (indicated by the white arrow). Reproduced with permission.[89] Copyright 2023, Springer Nature.

Polymeric-Based Electrode Modification: Conductive polymers have been extensively studied for their ability to enhance the stability and detection limits of biosensors.[70] Common examples include polypyrrole (PPy),[71] poly(o-phenylenediamine),[72] polyaniline,[73] and poly (3-hexylthiophene-co-3-thiopheneacetic acid) copolymer.[74] In one study, Mello and Mulato utilized polyaniline thin films immobilized with urease via a one-step galvanostatic method. This fabrication technique was more accessible and cost-effective compared to previously reported methods while delivering comparable results.[75] Another study by Kushwaha et al. produced a zinc oxide-encapsulated polyaniline-grafted chitosan composite. This biosensor demonstrated a response time of 3 min, a detection limit of 29.84 ppm, and storage stability of up to 8 weeks. The fabrication steps of this sensor are illustrated in **Figure 4a**.[76] Further research explored the use of poly(pyrrole-co-para-phenylenediamine) as a matrix for urease immobilization, yielding a biosensor with a fast response time of 10 s and a detection limit within the normal range of urea levels.[77]

However, one challenge with these polymers is achieving both a wide measuring range and a fast response time simultaneously. Guzinski et al. showed that using hydrophobic conducting polymers as solid contacts (SC) for an ion-selective membrane (ISM) enhanced biosensor performance.[78] Urbanowicz et al. fabricated a glassy carbon/polyazulene/NH^{4+} membrane for urease activity determination, achieving a short response

time (36 s), good stability (up to 60 days), and a detection limit of 220 μM.[68] Polymeric nanoparticles have also been reported to improve enzyme loading, resulting in rapid response times and low detection limits. Ondes et al. used poly(2-hydroxyethyl methacrylate-glycidyl methacrylate) nanoparticles to increase the loading capacity of urease. This biosensor exhibited exceptional performance, including a response time of 30 s, a detection limit of 0.77 μM, storage stability of up to 90 days, and high repeatability.[79] Additionally, some studies combined polymeric surfaces for enzyme immobilization with metals to enhance electron transfer. Situmorang et al. immobilized urease onto tungsten wire using a polymeric matrix, resulting in a biosensor with high sensitivity and specificity for urea. The device demonstrated a detection limit of 10 μM and a fast analytical time of 4 min.[80]

Carbon-Based Materials: Carbon-based materials, particularly graphene-based, are widely recognized for their exceptional properties, making them ideal candidates for urea biosensors. In a study by Nien et al., graphene oxide (GO)/nickel oxide (NiO) films modified with gold (Au) nanoparticles were employed for urea biosensing. GO enhanced electron transfer, while NiO contributed to improved catalytic properties. This biosensor demonstrated excellent selectivity for urea, a fast response time of 25 s, and a detection limit of 7.64 μM.[81] Another study by Bonini et al. developed a disposable biosensor specifically designed to monitor urea levels in dialysis patients. Reduced graphene oxide (rGO) was utilized as the matrix for enzyme immobilization and electron transfer. Compared to GO, rGO exhibited superior sensing properties, resulting in enhanced biosensor performance.[82]

Nanoparticles-Based Modifications: Nanoparticles have been extensively studied for their potential to enhance urea detection due to their unique properties, such as high surface area, catalytic activity, and stability. Jakhar and Pundir reported the preparation of aggregated urease enzyme nanoparticles using a green synthesis method. Jack beans were utilized for urease extraction and subsequent modification. This biosensor exhibited enhanced analytical performance, including high sensitivity, selectivity, a wide detection range, a low limit of detection (1 μM), excellent reproducibility, and storage stability for up to six months (Figure 4b).[83] Similarly, Wang et al. employed urease nanoparticles by producing Au/urease nanoparticles for urea detection at home. The formulation enhanced urease stability, and the results showed a high correlation with those obtained by high-performance liquid chromatography-mass spectrometry (HPLC-MS).[84] Magnetic nanoparticles have also been explored for urea biosensors. A study utilized graphene oxide nanoparticles integrated with urease magnetic beads, resulting in exceptional sensing properties, including a response time of 29 s and a detection limit of 1.338 mg dL^{-1}.[85] Moreover, biosensors fabricated with γ -Fe2O3 NPs nanoparticles (NPs)/graphene oxide (GO)/nickel oxide (NiO) exhibited high stability and a low detection limit of 7.91 μM.[86] Prajapati et al. developed manganese oxide nanoparticles (Mn_3O_4) using a green synthesis approach.[87] In another study, researchers designed a novel potentiometric urea sensor by manipulating the morphology of CuO nanostructures. By using mixed solvents to control nucleation and growth, they optimized CuO for urea detection. Immobilizing the urease enzyme onto CuO nanostructures enhanced the biosensor's performance, demonstrating a promising strategy for sensitive and selective urea detection in both medical and environmental applications.[88]

Despite the advantages of electrochemical methods for small molecule detection, they typically lack spatial information regarding the analyte, as detection occurs primarily around the sensing electrode. To address this limitation, Himori and Sakata developed a novel mobile sensing electrode combined with a wireless detection system. Their approach involved fabricating a conductive hydrogel motor with immobilized urease enzyme. The motor's movement was driven by surface tension changes induced by the interaction of urea with urease, producing NH_3 the NH_3-rich media reduces the surface tension thus keeping the motor away. medium reduced surface tension, propelling the motor. Wireless motion analysis was performed using impedance measurement and optical analysis (Figure 4c).[89] (**Tables 3** and **4**)

2.2. Non-Enzymatic Urea Biosensor

Enzymatic and non-enzymatic approaches each have their own advantages and limitations. The enzymatic approach, while offering high specificity and sensitivity, is hindered by the enzyme's high cost, limited stability, and the challenges associated with enzyme immobilization. To address these challenges, non-enzymatic approaches have gained attention. This method eliminates the use of enzymes and instead utilizes nanomaterials, primarily metals and metal oxides, to mimic enzymatic functions. Non-enzymatic biosensors provide improved stability and simpler fabrication processes due to the absence of biological components.[90] Among the various electroanalytical techniques employed for non-enzymatic urea detection, cyclic voltammetry (CV) is one of the most widely used. This technique involves applying a triangular potential waveform to an electrochemical cell equipped with a three-electrode system. The resulting current, as the potential sweeps across a range, is measured and plotted against the potential to generate a cyclic voltammogram. This graph provides information about the electrochemical behavior of the analyte.[91] Below is a summary of key studies that have focused on improving non-enzymatic urea biosensors by utilizing different material modifications.

2.2.1. Nickle-Based Materials

Metal nanostructures such as platinum, gold, and nickel have been studied for non-enzymatic urea detection due to their excellent electrocatalytic properties. However, Nickel-based materials have emerged as a popular choice for non-enzymatic urea detection due to their outstanding electrocatalytic properties, cost-effectiveness, and ability to support diverse sensor designs. These materials address key challenges associated with enzymatic sensors, such as instability and high costs, while offering high sensitivity, low detection limits, and good repeatability. Several studies have explored innovative nickel-based composites to enhance the performance of urea biosensors.[92] One notable approach involves the synthesis of nickel cobalt oxide nanoneedles by Amin et al. These nanostructures were designed to optimize the electric properties of metal oxides by controlling their

Table 3. Comparison in analytical characteristics for various enzymatic potentiometric urea biosensors.

	ELECTRODE/mATERIAL	MATRIX TYPE	IMMOBILIZATION METHODS	dETECTION LIMIT (LOD)/SENSITIVITY	RESPONSE TIME	REUSABILITY/sTORAGE STABILITY	REFERENCES
1	Pt electrode	Polyaniline thin films	-	7.4 ± 0.5 mV decade^{-1}	-	-	[69]
2	Bioelectrode	ZnO /polyaniline/ chitosan	Glutaraldehyde	29.84 ppm 187.5 μV/(ppm.cm2)	3 min	8 weeks	[70]
3	Stainless steel electrode	Poly (Pyrrole-co-Para-Phenylenediamine)	Covalent immobilization	0.5–10.0 мм 47.3–54.2 mV/pUrea	10 s		[71]
4	Glassy carbon electrode	Glassy carbon/polyazulene/ NH^{4+} membrane	-	220 μм	36 s	60 days	[73]
5		Poly (2-hydroxyethyl methacrylate glycidyl methacrylate) NPs	-	0.7 μм	30 s	90 days	[74]
6		Polymeric matrix / W wire		10 μм	4 min		[75]
7		GO/NiO / Au NPs.		7.64 μм	25 s		[76]
9	AISE	Urease NPs		1 μм 23 mV	10 s	8–9 times a day over 180 days- storage 4 °C	[78]
9	Au /Pt electrode	Au@urease Nanoparticles					[68]
10		GO nanoparticles		1.338 mg dl^{-1}	29 s		[79]
11	Silver wire/ (PET) substrate	GO / γ-Fe_2O_3 NPs		7.91 μм 52.36 mV decade^{-1}			[80]

Table 4. Comparison in analytical characteristics for various non-enzymatic urea biosensors.

	TYPE OF MATERIAL USED	SENSITIVITY	DETECTION LIMIT	RESPONSE TIME	STORAGE/ rEPRODUCIABILIY	REFERENCES
1	Copper phthalocyanine	16.43 μA(мм.cm^2)	0.05 μм			[90]
2	NiO molybdenum trioxide	N/A	0.86 μм	Not reported		[82]
3	Nickle cobalt oxide nanoneedle	N/A	1 μм	Not reported	66% activity 1 мм of urea	[83]
4	Ni/Au electrode	52.2 мм/(μAcm^2)	33.5 μм	Not reported	RSD% of 0.12% after 9 days	[84]
5	2D MOF	1960 μA/(ммcm^2)	0.471 μм	2 s	RSD%: 3.3%	[85]
6	NS/GO	N/A	3.79 μм	Not reported	Recovery %: 98.6–99.4%. Same performance 10 cycles	[86]
7	NiS/GO	5139.2 μA.мм/(cm^2)	7 μм	Not reported	92% of the initial response (after 30 days)	[87]
8	$Ni(OH)_2/Mn_3O_4$ /rGO/PANI	32.6 μA. L mmol^{-1}	16.3 μм			[88]
9	Ag / NiO	N//A	8 μм			[89]
10	SWCNTs	N/A	0.0047 μм	3 s	Not reported	[92]
11	NiO	N/A	4 μм			[93]
12	NiO NPs/ GO GCE	N/A	8 μм			[94]
13	K-carrageenan/PVA/nano-eggshell	0.018 μA.mM/(cm^2)	60 μм	Not reported		[95]

size and shape. To overcome limitations like low conductivity and poor charge transfer, a bimetallic 1D nanosystem was developed. This material outperformed enzymatic sensors, achieving a detection limit as low as 1 μм.[93] Similarly, a nickel oxide-molybdenum trioxide nanocomposite, prepared through a hydrothermal method, demonstrated an even lower detection limit of 0.86 μм, surpassing the performance of many previously reported materials.[94] Tahira et al. developed a urea sensor utilizing $NiCo_2O_4$ nanowires synthesized with polyvinylpyrrolidone (PVP) as a structure-directing agent. The $NiCo_2O_4$ nanowires exhibited exceptional electrocatalytic activity, enabling highly sensitive and selective urea detection. The sensor demonstrated a wide linear detection range, a low detection limit, and remarkable stability, making it a promising alternative to conventional

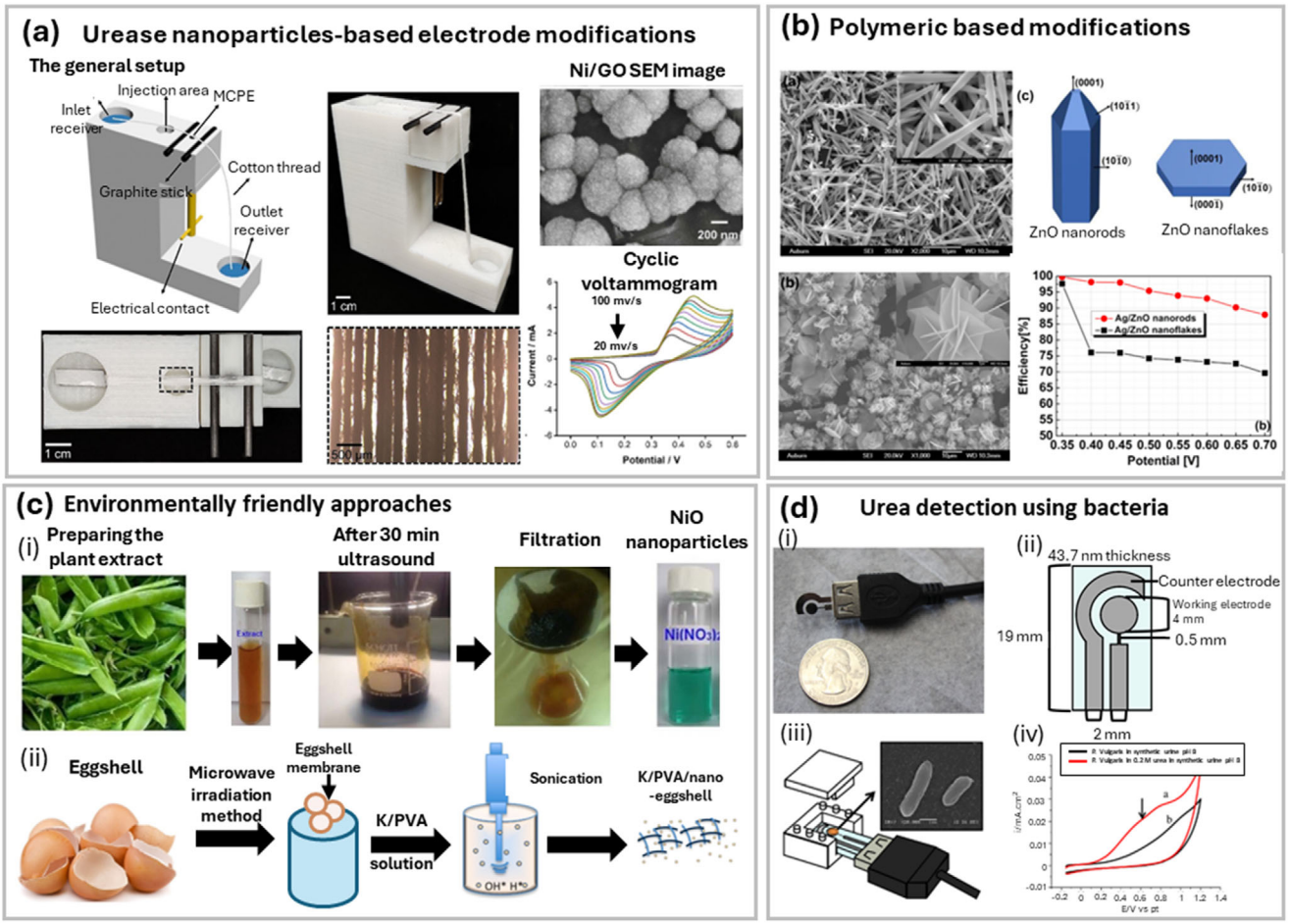

Figure 5. Advances in Non-Enzymatic Urea Biosensors. a) Schematic representation of a non-enzymatic urea biosensor utilizing graphene oxide (GO)/Ni nanoparticles. This device detects urea from saliva as it flows through a cotton thread, reaching an electrode coated with GO/Ni. Urea detection occurs upon voltage application, enabling real-time analysis. Reproduced with permission.[80]. b) Effect of nanoparticle shape on the overall performance of a ZnO/Ag nanocomposite-based urea sensor. The morphology of nanomaterials plays a crucial role in sensor sensitivity and efficiency. Reproduced with permission.[106] Copyright 2019, Wiley. c) Overview of different environmentally friendly approaches for producing materials suitable for urea detection. Sustainable fabrication methods are explored to enhance sensor performance while minimizing environmental impact. (i) presents NiO nanoparticles produced from a plant extract. Reproduced with permission.[110] Copyright 2018, Elsevier. Whereases (ii) shows a different way to produce nanoparticles using eggshell. Reproduced with permission.[111] Copyright 2020, Springer Nature. d) Custom Pt miniature electrode chip images illustrating: (i) Size comparison and connector (ii) Chip design (iii) Electrochemical setup: P. vulgaris on working area, connected via USB cable. (iv) Cyclic voltammograms for indirect urea detection via ammonia oxidation. Reproduced with permission.[114] Copyright 2019, Elsevier.

enzymatic urea sensors for clinical diagnostics and environmental monitoring.[95]

Irzalinda et al. further advanced the field by developing a Ni/Au electrode. Nickel was chosen for its superior catalytic properties and affordability. The resulting sensor exhibited excellent repeatability and stability, maintaining its performance for nine days without significant changes. The sensor also showed a detection limit of 33.5 μM and demonstrated high selectivity in the presence of interfering substances.[96] In another study, Wang et al. fabricated 2D metal-organic frameworks (MOFs) using Co, NiCo, and Ni nanosheets. Among these, Ni-MOF showed the highest sensitivity with a detection limit of 0.471 μM and a rapid response time of just two seconds.[97] Graphene-based nanocomposites have also been employed to enhance the properties of nickel-based materials. For example, a nickel sulfide/graphene oxide (NiS/GO) composite was fabricated to improve electron transfer and stability. This composite demonstrated excellent electrocatalytic behavior, with a low detection limit of 3.79 μM and high reusability, achieving a recovery rate of 98.6–99.4%.[98] Another advanced sensor, made of $Ni(OH)_2/Mn_3O_4$/rGO/PANi, showcased impressive stability, anti-interference properties, and a detection limit of 16.3 μM.[99]

Nickel-based materials have also shown potential for non-invasive urea detection. For instance, a NiS/GO sensor was adapted for urea detection in saliva, making it suitable for point-of-care (POC) testing. This device, integrated with a microflow injection analysis (FIA) system, exhibited a detection range of 0.1–6 mM and a limit of detection (LOD) of 7.02 μM.[100] **Figure 5a** shows how the basic concept of amperometry can be applied to fabricate a simple device usable for POC. Similarly, Abdollahi and Mashhadizadeh developed a wearable sensor for urea detection in sweat. By modifying a carbon electrode with silver-doped

nickel oxide and incorporating it into a non-woven fabric, they created a textile electrode with a detection limit of 8 μM and high sensitivity and stability, paving the way for wearable and non-invasive urea monitoring applications.[101]

2.2.2. Other Metal and Metal Oxide-Based Materials

Other metals and metal oxide-based materials have demonstrated significant potential for non-enzymatic urea detection, offering high sensitivity, selectivity, and stability. One notable example is the work by Güngör et al., who fabricated copper phthalocyanine (CuPc)-borophene nanocomposites using a sonochemical approach. The combination of CuPc, an aromatic dye, and borophene, a 2D boron nanostructure with exceptional charge transfer properties, resulted in a biosensor with high selectivity across various matrices and excellent sensitivity even in the presence of competitive ions. This sensor achieved a detection limit of 0.05 μM, demonstrating the synergistic effects of CuPc and borophene in enhancing detection performance.[102] Magar et al. developed a non-enzymatic, disposable electrochemical sensor for direct urea detection, utilizing a CuO/Co_3O_4@MWCNTs nanocomposite-modified screen-printed electrode. The nanocomposite, composed of copper oxide (CuO), cobalt oxide (Co_3O_4), and multi-walled carbon nanotubes (MWCNTs), exhibited excellent electrocatalytic activity toward urea oxidation.[103] In another study, Ray et al. designed enzyme-free urea sensors using oyster pearl-shaped $FeSe_{0.5}Te_{0.5}$ films electrochemically grown on FTO substrates. The unique ternary iron chalcogenide structure enhanced electrocatalytic activity, enabling highly sensitive and selective urea detection in real samples. The sensor demonstrated excellent performance, positioning it as a promising candidate for clinical and environmental monitoring.[104]

Silver-based materials have also been extensively studied for their catalytic properties in urea detection. Kumar and Sundramoorthy developed a nanocomposite by decorating nitrogen-doped single-walled carbon nanotubes (SWCNTs) with silver nanoparticles (Ag-NPs) using a one-step thermal reduction method. This composite significantly outperformed SWCNTs alone, providing high catalytic activity, sensitivity, and a detection limit of 0.0047 μM. Additionally, the sensor exhibited excellent selectivity, repeatability, stability, and a fast response time of just three seconds.[105] In a further development, a study reported the use of silver-coated zinc oxide (ZnO) with different nanostructures, such as nanorods and nanoflakes, for urea detection. Among these, ZnO nanorods demonstrated superior catalytic properties due to their higher electrochemical surface area, which facilitates faster electron transfer. This finding highlights the importance of nanostructure morphology in optimizing the performance of non-enzymatic urea sensors, as illustrated in Figure 5b.[106] Additionally, a silver/PANI composite provided an efficient and cost-effective approach for urea detection[107] Khataee et al. developed a non-enzymatic urea sensor utilizing La-doped CoFe-layered double hydroxide on reduced graphene oxide (rGO). This nanocomposite demonstrated superior electrocatalytic activity for urea oxidation by leveraging the benefits of La doping and the high conductivity of rGO. The sensor exhibited high sensitivity, a wide linear detection range, and a low detection limit, making it a promising tool for urea monitoring in clinical and environmental applications.[108]

2.2.3. Environmentally Friendly Approaches Based on Metal Oxides

Metal oxides have gained significant attention in developing environmentally friendly approaches for non-enzymatic urea detection. Despite the remarkable properties of nickel-based materials, many production methods lack environmental sustainability, cost-effectiveness, and scalability. To address this, green chemistry techniques have been explored. For instance, NiO-based nanomaterials were produced using a combined green and chemical method where nickel oxide nanostructures were stabilized in a plant extract substrate derived from rice straw. The resulting material exhibited excellent redox ability, stability, rapid response time, and a low detection limit of 4 μM. These enhanced properties were attributed to fast charge transfer, numerous active sites, and a high surface area.[109] Similarly, Parsaee reported a green method to modify urea biosensors, fabricating NiO nanoparticles on a graphene oxide (GO)-modified glassy carbon electrode. Nickel oxide nanoparticles were synthesized from a *Pisum sativum* plant extract. Nickel was chosen for its low toxicity, cost, and stability, but its poor electrical conductivity was addressed by combining it with GO. GO not only facilitated better electron transfer but also provided additional active sites to prevent nanoparticle agglomeration. The resulting biosensor showed a detection limit of 8 μM, exceptional selectivity against interfering substances, and eliminated the need for special storage conditions.[110] In another innovative study, a novel biosensor was developed using K-carrageenan/PVA/nano-eggshell via the ultrasonic sonochemical approach. This biosensor demonstrated impressive performance with a detection limit of 60 μM and a sensitivity of 0.018 $\mu A\ \mu M^{-1}\ Cm^{-2}$, showcasing the potential of sustainable materials for efficient urea detection.[111] Additionally, Yadav et al. reported a novel approach for urea detection using a compost-based microbial fuel cell (MFC) with a tin oxide nanoparticle-coated cathode. This dual-purpose system not only detects urea but also generates energy, outperforming conventional electrodes. While primarily designed for environmental applications, technology holds potential for biomedical adaptations, such as urine analysis. Notably, this is the first reported urea sensor utilizing an MFC configuration.[112]

2.2.4. Urea Detection Using Bacteria

Bacteria-based approaches have also been explored for urea detection, leveraging microbial enzymatic activity to indirectly monitor urea levels. For example, Ariyanti et al. developed a urea biosensor using whole cells of *Bacillus licheniformis* to detect urea in artificial urine. Urea detection was achieved indirectly through the ammonia oxidation reaction catalyzed by *B. licheniformis*. This system employed a three-electrode setup with screen printing and demonstrated a detection limit of 0.01 M, a linear detection range of 0.01–0.2 M, and a sensitivity of 1.278 $\mu A\ M^{-1}$.[113] In another study, a lab-on-a-chip sensor was developed to detect urea in synthetic urine by measuring the electrochemical oxidation of ammonia. The ammonia was produced through the enzymatic activity of the microbial organism Proteus vulgaris on

urea. The sensor demonstrated a correlation between the peak current density of ammonia oxidation (ranging from 0.5 to 5.0 μA cm^{-2}) and urea concentration (ranging from 0.01 to 0.1 M) in synthetic urine. Using sample volumes of 80 and 100 μL at pH 8.0, the smaller volume exhibited reduced variability and higher sensitivity.[114] These studies highlight the potential of microbial systems for innovative and efficient urea detection methods.

3. Key Technological Advancements

3.1. Enhanced Sensitivity and Selectivity

Sensitivity is a critical parameter in biomedical applications, particularly for analyte detection. This is especially true for substances like urea, which are present in trace amounts. To be effective, biosensors must detect these analytes at low concentrations with precision, even in the presence of interfering substances. Numerous urea biosensors with improved sensitivity and linearity have been developed by researchers.[82,115–118] However, conventional electrochemical measurement systems face limitations as their miniaturization reduces the signal-to-noise ratio, making it challenging to accurately detect urea at low concentrations As for practical applications, a signal-to-noise ratio (SNR) of a minimum of 3:1 is necessary for detection, however an SNR of 10:1 or greater is advised for dependable quantification in clinical contexts.[119–122] To enhance sensitivity, modifications to the electrode are often necessary to facilitate faster diffusion of redox species.[123] For instance, Senel et al. devised a straightforward and efficient method to fabricate an array of gold microneedles (AuMNs) by casting conductive gold ink. These AuMNs were coated with a polymer containing epoxy and ferrocene groups, followed by the attachment of urease. This biosensor demonstrated excellent performance, with a detection range of 50–2500 μM, a detection limit of 2.8 μM, and a sensitivity of 31 nA mM^{-1}.[124] **Figure 6a** shows the production steps of gold microneedles used to enhance the sensitivity of the biosensor. In another study, Rahmanian et al. constructed a 3D hierarchical Nano-ZnO/TiO_2 layer on a conductive fluorinated-tin oxide (FTO) substrate. TiO_2 was selected as the base material due to its ability to support electron transfer between ZnO and FTO while forming a heterojunction with ZnO to enhance biosensing properties. Additionally, TiO2 increased the electronic density on the biosensor surface, improving electron transfer. Using impedimetric assessment, the biosensor achieved a high sensitivity with a detection range of 5–205 mg dL^{-1} and a detection limit of 2 mg dL^{-1}.[125]

Low detection limits have also been achieved through non-enzymatic approaches. For example, ultrathin nickel-metal–organic framework (Ni-MOF) nanobelts developed for urea detection in alkaline conditions exhibited remarkable performance, including a sensitivity of 118.77 mA mM^{-1} cm^{-2}, a broad detection range of 0.01–7.0 mM, and a detection limit of 2.23 μM.[126] Yoon et al. synthesized a nickel-based material, Ag/NiOOH nanorod composite, capable of detecting urea across different pH levels. This material showed a high sensitivity of 233.7 μA mM^{-1} cm^{-2}, a wide linear range of 0.2–26.0 mM, a rapid response time of ≈3 s, and a detection limit of 5.0 μM.[127] Another notable study employed a one-pot solvothermal method to produce a zeolitic imidazolate framework (Co-ZIF) combined with nickel microwires (NiMWs), which were subsequently deposited on a glassy carbon electrode. The resulting biosensor exhibited outstanding properties, including a broad detection range of 0.5×10^{-6} to 0.5×10^{-3} M, a remarkably low detection limit of 0.3×10^{-6} M, and excellent selectivity and sensitivity.[128]

3.2. Miniaturization and Portability

Personalized medicine often faces challenges such as the need for minimally invasive biomarker monitoring. Wearable and portable devices are pivotal in addressing these challenges.[129–131] For example, Liu et al. developed an affordable and portable device for urea detection using electrochemistry. This was achieved by modifying a commercial glucose test strip with silver nanoparticles (AgNPs). The strip's enzymes were removed, and AgNPs were deposited onto the working electrode. The device demonstrated a detection range of 1–8 mM, aligning with physiological levels in human blood, and a detection limit of 0.14 mM.[132] Another study fabricated a flexible urea biosensor using molecularly imprinted nanotubes via electro-polymerization. The biosensor exhibited an impressive dynamic detection range of 1–100 mM.[133] Figure 6b represents flexible urea biosensor fabrication: schematic, performance curves, and sensor response stages (electropolymerization, elution, adsorption). Similarly, Kim et al. developed a sensor incorporating a porous silk fibroin membrane immobilized with urease, housed in a polydimethylsiloxane (PDMS) structure. This sensor demonstrated linear current-concentration characteristics within the clinical range (0.1–20 mM).[134] Notably, their study tested urea levels under dynamic conditions using microfluidics, which replicate fluid flow, such as blood circulation, and requires minimal sample volume. Despite the significance of dynamic testing, only a few studies focus on developing wearable urea sensors under such conditions.[135–139]

Since sweat is a readily accessible body fluid that encounters the skin, many studies have explored its use for urea detection. For instance, Ibáñez-Redín et al. developed a potentiometric urea biosensor using screen-printed electrode arrays with polyaniline (PANI) nanoparticles and urease-containing bio-ink in a polyvinyl chloride membrane. The biosensor included a pH sensor to account for variations in sweat pH, enabling precise detection across a wide range (5–200 mM) with a rapid response time of 5 min.[140]

In another study, Ashakirin et al. utilized a label-free detection approach by modifying a working electrode with a silver-rGO nanocomposite, which served as a matrix for urease immobilization. The miniaturized electrodes, produced using screen printing, demonstrated exceptional performance with high selectivity for urea, a sensitivity of 47.598 μA $μM^{-1}$ cm^{-2}, a wide linear detection range (0.001–10 mM), and a detection limit of 0.1623 μM.[141] Further advancements include the development of a biosensor utilizing cyclic voltammetry. A NiCu(OOH)/polystyrene (PS) electrode was fabricated through electrospinning, with carbon nanotubes as the conductive element. Nickel-copper alloy, introduced via co-sputtering, acted as a catalyst. The sensor exhibited a detection range of 2–30 mM with minimal interference from other substances. Its excellent performance was attributed to the porous structure of PS, which provided more active sites and improved water wettability, facilitating charge transfer.[142] Roy et al. created a novel non-enzymatic electrochemical sensing chip for

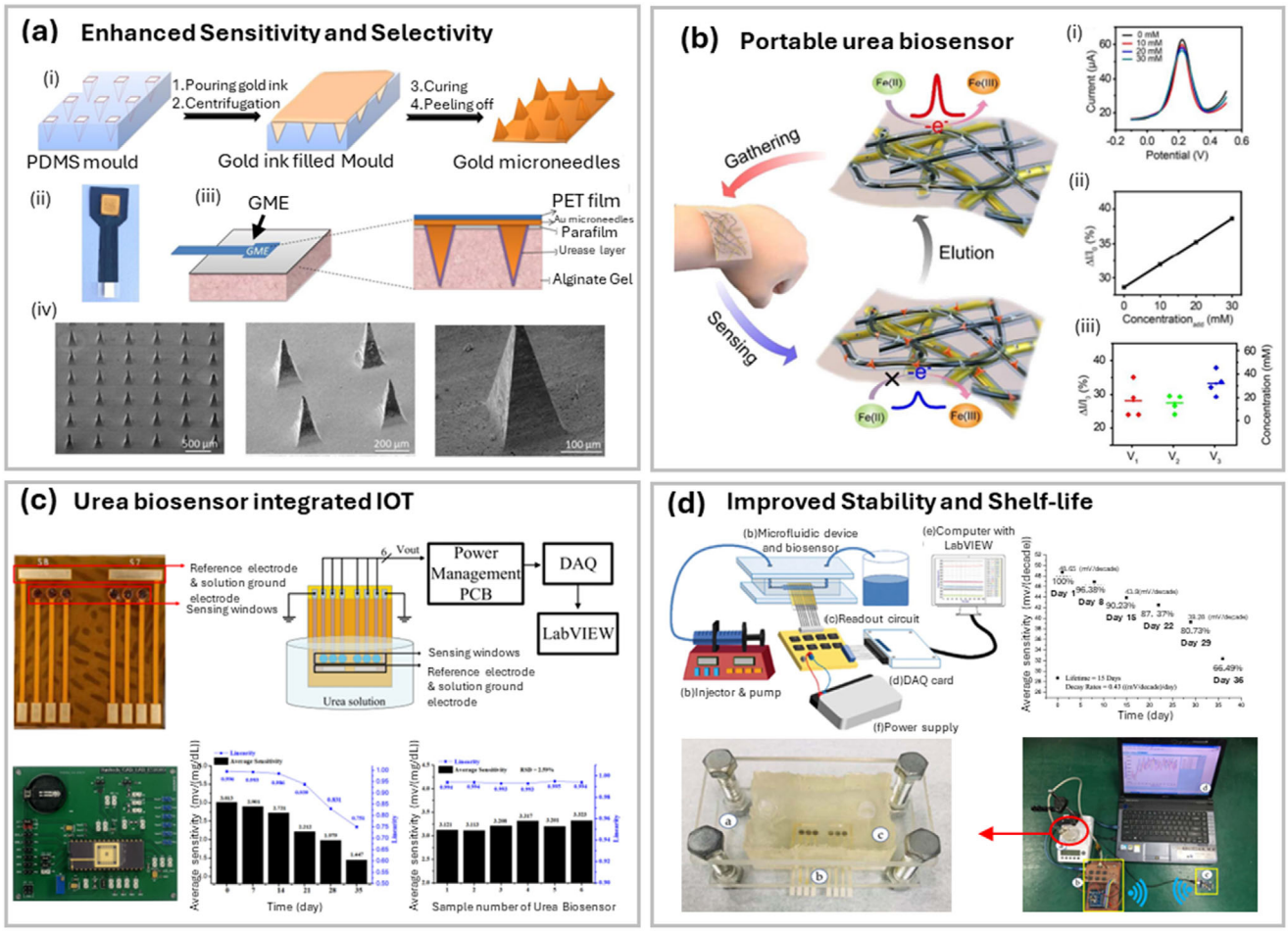

Figure 6. Innovations in Urea Biosensor Fabrication and Performance Evaluation a) Microneedle-Based Urea Sensor: (i) Production steps for gold microneedles. (ii) Optical image of the sensor's working electrode. (iii) Schematic illustration of urea detection utilizing a nonporous Parafilm barrier and alginate hydrogel. (iv) SEM images of gold microneedles. Reproduced with permission.[124] Copyright 2019, Elsevier. b) Flexible Urea Biosensor Fabrication: represents a schematic of the flexible urea biosensor fabrication. (i) Potential versus current curves for different urea concentrations. (ii) Calibration curve demonstrating the biosensor's response with increasing urea concentrations. (iii) Sensor response at different stages: electropolymerization (green), elution (red), and adsorption (blue). Reproduced with permission.[133] Copyright 2018, ACS Publications. c) Schematic representation of the arrayed flexible printed circuit board (FPCB) RuO_2-based biosensor, including the general experimental setup. Data illustrating biosensor reproducibility and operational lifetime. Reproduced with permission.[167] Copyright 2023, IEEE Access. d) Experimental setup of a microfluidic urea biosensor system comprising an injector and pump, microfluidic device, biosensor, readout circuit, DAQ card, computer, and power source. The figure represents the biosensor's operational lifetime. Reproduced with permission.[171] Copyright 2024, Springer Nature.

point-of-care (PoC) urea detection in human blood. The chip, made using 3D-printed conductive silver ink coated with a gold nanoparticle-reduced graphene oxide (AuNP-rGO) nanocomposite, showed high sensitivity (183 µA mM^{-1} cm^{-2}), a low detection limit (0.1 mM), and rapid response due to a high diffusion coefficient. With a shelf life exceeding six months and a recovery rate of over 99%, the chip is highly suitable for PoC urea detection kits.[143] Lastly, Nhu et al. developed a miniaturized potentiometric urea sensor using the LMP9 1000 integrated circuit. The device comprised three components: an electrode, an electrochemical measuring circuit, and a data acquisition unit. Non-enzymatic urea detection was achieved using cobalt sulfide (CoS) materials by assessing changes in oxidation potential peaks at 100 mV. The sensor exhibited a linear detection range of 1–8 mM, corresponding to physiological blood levels, and a sensitivity of 7.5 µA mM^{-1} cm^{-2}, comparable to other studies.[144] Dervisevic et al. developed a wearable microneedle biosensor with recessed microcavities for non-invasive urea monitoring in interstitial fluid. The device demonstrated high sensitivity (2.5 mV mM^{-1}) and a linear range of 3–18 mM, proving effective in ex vivo tests. This innovation presents a promising alternative to traditional blood-based diagnostics for personalized health monitoring.[145] Furthermore, Abad et al. introduced a self-powered urea biosensor designed for human energy harvesting. This biosensor utilizes urea as a biofuel to generate energy, enabling continuous monitoring without external power sources. A predictive evolutionary model was developed to optimize its performance and energy efficiency. This novel approach holds significant potential for wearable health monitoring and sustainable energy solutions in personalized medicine.[146]

Continuous monitoring of urea levels is critical for patients with chronic kidney disease and other metabolic disorders, as

it enables timely intervention and better disease management. Electrochemical urea biosensors, particularly those based on enzymatic and non-enzymatic approaches, offer promising solutions for real-time tracking due to their rapid response, high sensitivity, and potential for miniaturization. Enzymatic biosensors typically utilize urease immobilized on electrode surfaces to catalyze urea hydrolysis, producing ammonium and bicarbonate ions that are detected via amperometric or potentiometric methods. These platforms can be integrated into wearable devices or microfluidic systems for dynamic sampling and analysis under physiological conditions.[46,82,134] For instance, Bonini et al. developed a disposable biosensor capable of real-time urea monitoring during dialysis, demonstrating a response time of 120 seconds and strong correlation with clinical methods.[82] Similarly, Kim et al. fabricated a microfluidic biosensor using urease immobilized on a silk fibroin membrane, enabling continuous detection in flowing fluids with high accuracy.[134] Non-enzymatic sensors, leveraging nanomaterials such as $NiCo_2O_4$ or Ag/NiOOH composites, further enhance stability and reduce cost, making them suitable for long-term monitoring applications.[127,101] These biosensors can be embedded into flexible substrates or textile-based electrodes for non-invasive detection in sweat or saliva, supporting continuous health tracking outside clinical settings. The integration of electrochemical biosensors with wireless electronics and IoT platforms further facilitates real-time data acquisition and remote monitoring, paving the way for personalized diagnostics and point-of-care applications.[164]

3.3. Integration with Digital Technologies

The demand for point-of-care (PoC) urea detection integrated with smartphones has been growing due to its affordability, ease of use, and ability to provide quick, on-site results. Several biosensors have been developed using optical, surface plasmon resonance, and electrochemical approaches, with the electrochemical approach standing out for its high selectivity toward specific analytes.[147–150] However, reports of electrochemical urea biosensors integrated with smartphones are limited compared to those for other analytes like glucose,[151–153] creatinine,[154–156] and albumin[157–159] Most smartphone-integrated urea biosensors rely on colorimetric or optical methods,[139,160–163] Liu et al. addressed this gap by developing a screen-printed electrode based on MXene (titanium carbide) integrated with a dialysis microfluidic chip. This device allows direct and continuous analysis of multiple blood components, including urea, uric acid, and creatinine. By incorporating a ratiometric sensing approach, signal drifting was minimized. The device achieved a detection range of $0–3 \times 10^{-3}$ M and a detection limit of 0.02×10^{-3} M for urea.[164] Despite such advancements, there remains a need for miniaturized electrochemical urea biosensors to complement these developments. Mello et al. compared the electrochemical and optical responses of enzymatic biosensors. They examined electrochemical impedimetric and capacitive responses for the first time and compared them to optical reflectance responses measured using a portable spectrophotometer. Sensors fabricated using polyaniline thin films functionalized with enzymes demonstrated detection ranges of 10^{-4} to 10^{-1} mol L^{-1} for glucose and urea, with detection limits ≈1 µmol L^{-1}. These features underscore their practicality for biomedical applications.[165] While urea biosensor integration with smartphones or IoT remains underexplored, advancements in other smartphone-integrated devices provide insights for future development. For instance, Larpant et al. demonstrated a battery-free sensor design for redox detection in biological samples. Their approach incorporated silver nanoparticles (AgNPs) into RFID tag antennas, where horseradish peroxidase (HRP) enzymes converted AgNPs into AgCl in the presence of hydrogen peroxide, altering the tag's impedance. Gold nanoparticles (AuNPs) facilitated electron transfer between the AgNPs and HRP, enabling the creation of battery-free biosensor-RFID tags for detecting hydrogen peroxide and glucose. This method holds promise for adapting similar sensors for other redox reactions involving oxidoreductase enzymes, bacteria, or non-biological catalysts.[166] Efforts to miniaturize and enhance urea biosensors for practical applications have also been reported by Kuo et al. They designed a printed circuit board (PCB) combining a power management circuit with a readout circuit, powered by a 3 V button cell. This design supports voltage reduction and stabilization. Using radio frequency sputtering, RuO_2 was printed on a flexible PCB for enzyme-based urea detection. The sensor achieved an average sensitivity of 3.121 mV/(mg dL^{-1}), linearity of 0.994, and reproducibility of 2.59% Figure 6c represents a schematic of the arrayed flexible printed circuit board biosensor using RuO_2, along with its experimental setup.[167] Prabhu et al. introduced an innovative impedimetric biosensing system integrated with IoT for real-time kidney health monitoring. This point-of-care (PoC) biosensor enables rapid detection of creatinine levels in urine or serum, serving as a key indicator of kidney function. Offering both qualitative and quantitative assessments, the system enhances prognostic and prophylactic care for kidney disease patients. The IoT integration further enables remote monitoring and data management, improving accessibility and clinical utility.[168]

3.4. Improved Stability and Shelf-Life

Stability is a critical feature of biosensors but is seldom discussed in the literature.[135] Stability analysis typically evaluates the degree of interference within the biosensor system, which can arise from factors like thermal interference affecting the output signal and bond strength between the sensing film and the analyte. Enhancing stability often involves employing covalent bonding techniques. Additionally, stability is assessed by examining repeatability and performance under varying conditions, such as high temperatures.[169–172] Kuo et al. investigated the stability of a potentiometric biosensor designed for urea detection. They fabricated the sensor using a urease-Ag nanoparticle/Ruthenium dioxide (RuO_2) sensing film. RuO_2 is widely favored for its thermodynamic and chemical stability, high conductivity, and excellent catalytic properties. The biosensor's stability was assessed by measuring its reproducibility, repeatability, and long-term performance using a microfluidic wireless measurement system. The results demonstrated high reproducibility (RSD = 2.23%) and repeatability (RSD = 1.16%) across a broad urea concentration range (0.005–50 mg dL^{-1}). Additionally, the sensor exhibited exceptional sensitivity and linearity at temperatures ranging from 25 to 65 °C. Remarkably, the device retained 90% of its initial sen-

sitivity after 15 days of storage at room temperature and achieved an accuracy of 94.70% in remote measurement applications.[135] One critical factor influencing a biosensor's accuracy, reusability, and stability is the hysteresis effect. Hysteresis occurs when the output voltage differs from its initial value after a urea concentration change returns to the starting level, leading to potential instability and response variations. To address this, Kuo et al. developed methods to minimize the hysteresis effect in potentiometric urea biosensors. They proposed a novel analog back-end circuit with a voltage regulation mechanism and utilized RuO_2 thin film combined with Ag/urease nanoparticles for redox reactions. Experimental findings revealed an average sensitivity of 48.73 mV decade^{-1} and a linearity of 0.996 over a wide urea concentration range (0.833 μM to 8.33 mM). The sensor achieved a fast response time of 22 s and a detection limit of 0.37 μM. Furthermore, the hysteresis voltage was reduced by 29%, from 3.71 to 2.62 mV[173] represnts the setup for a microfludic system for urea biosensor. Nien et al. reported a urea biosensor based on a graphene oxide/nickel oxide sensing film, modified with either Au nanoparticles or γ-Fe_2O_3 nanoparticles. To improve the sensor's performance, the researchers developed a back-end calibration circuit that effectively reduces drift and hysteresis effects. This approach enhances the stability and reliability of the biosensor, ensuring more accurate urea measurements across various applications.[174]

4. Applications in Medical Diagnostics and Biomedical Fields

4.1. Renal Disease Detection

Kidney diseases are often diagnosed by abnormal concentrations of biomarkers such as urea, uric acid, C-reactive protein, and creatinine.[175–178] Elevated serum urea levels, in particular, are indicative of kidney failure or impaired glomerular filtration rate. Traditional methods for detecting kidney disease rely on measuring these biomarkers in blood, urine, or other body fluids, primarily focusing on urea and creatinine.[179,180] Historically, urea levels have been quantified using calorimetric techniques, such as the phenol-hypochlorite and Nesslerization methods,[3] alongside other approaches like chemiluminescence, colorimetry, spectrophotometry, and fluorimetry. While spectroscopic methods remain the standard in most laboratories, these techniques are often labor-intensive, time-consuming, and require specialized equipment and trained personnel, limiting their cost-effectiveness.[181,182]

To address these challenges, biosensors have emerged as a promising alternative. For example, Kumar et al. developed a nano-bioengineered electrode using Ag-complex-based quaternary Ag–S–Zn–O nanocomposites. These materials were chosen for their small size and high surface area-to-volume ratio, enhancing the biosensor's sensitivity and selectivity. By immobilizing urease on the electrode, the biosensor achieved high sensitivity (12.56 μA mM^{-1} cm^{-2}) and a low detection limit of 0.54 mM. Additionally, the biosensor demonstrated excellent reproducibility, stability for up to 60 days, and potential for clinical application **Figure 7a** represents the preparation, characterization, performance and mechanism of action of electrodes made of silver-sulfur-zinc-oxide nanocomposites.[183] Another study introduced a urea biosensor using poly(2-hydroxyethyl methacrylate-glycidyl methacrylate) nanoparticles as enzyme carriers. Tested with artificial human serum, the biosensor exhibited a linear detection range of 0.01 to 500 mM, a detection limit of 0.77 μM, and a response time of 30 s. Remarkably, the device retained 95.7% of its performance after 170 uses and 83% of its activity after 90 days of storage, highlighting its suitability for clinical applications.[79]

Despite these advancements, the use of electrochemical approaches in clinical diagnostics remains limited. Bonini et al. developed a disposable biosensor specifically for real-time urea monitoring during dialysis for end-stage kidney disease patients. This device utilizes a pH-sensitive reduced graphene oxide layer functionalized with 4-amino benzoic acid and urease. Upon catalyzing the breakdown of urea, the sensor detects pH changes, enabling accurate potentiometric measurements. Tested on plasma samples from dialysis patients, the biosensor demonstrated a response time of 120 s and an error margin of 6 ± 3% compared to standard clinical methods.[82] Other innovative approaches include pH-based detection systems. For instance, Soni et al. designed a portable biosensor integrated with a smartphone application to measure urea levels in saliva. This device employs a urease enzyme immobilized on a filter paper strip with a pH indicator. Upon exposure to urea, the strip changes color, and the resulting RGB profile is analyzed via a smartphone app. Validation with spiked saliva samples and healthy volunteers revealed a linear detection range of 10–260 mg dL^{-1}, a response time of 20 s, and a sensitivity of -0.005 average pixels per second per mg dL^{-1}. The biosensor also demonstrated a detection limit of 10.4 mg dL^{-1}.[139]

4.2. Clinical Diagnosis, Point-of-Care, and Portable Applications

Clinical diagnostics demand rapid and accurate analytical methods, particularly for point-of-care (POC) testing.[184] To meet this need, researchers are developing user-friendly biosensors capable of detecting target analytes with high specificity.[185] One notable study by Berto et al. introduced a urea biosensor utilizing urease encapsulated within a cross-linked gelatin hydrogel, integrated into a fully printed PEDOT:PSS-based organic electrochemical transistor (OECT). This sensor detects changes in channel conductivity resulting from ionic species generated during urease-catalyzed urea hydrolysis. The biosensor demonstrated outstanding reproducibility, with a detection limit of 1 μM and a rapid response time of just a few minutes. Manufactured using screen-printing on flexible substrates, the OECTs offer low production costs and fast turnaround times. The device's compact size and low operating voltage (0.5 V or less) make it particularly suited for high-throughput POC urea monitoring and field applications.[186] In another study, Liu developed a cost-effective and portable platform for urea detection using electrochemical methods. This involved modifying commercial glucose test strips by removing surface enzymes and electrodepositing silver nanoparticles (AgNPs) onto the working electrode. Scanning Electron Microscopy (SEM) was used to analyze the modified strip's morphology, while Cyclic Voltammetry (CV) and Electrochemical Impedance Spectroscopy (EIS) assessed its electrochemical performance. The biosensor exhibited a linear detection range of 1–8 mM, corresponding to the physiological urea

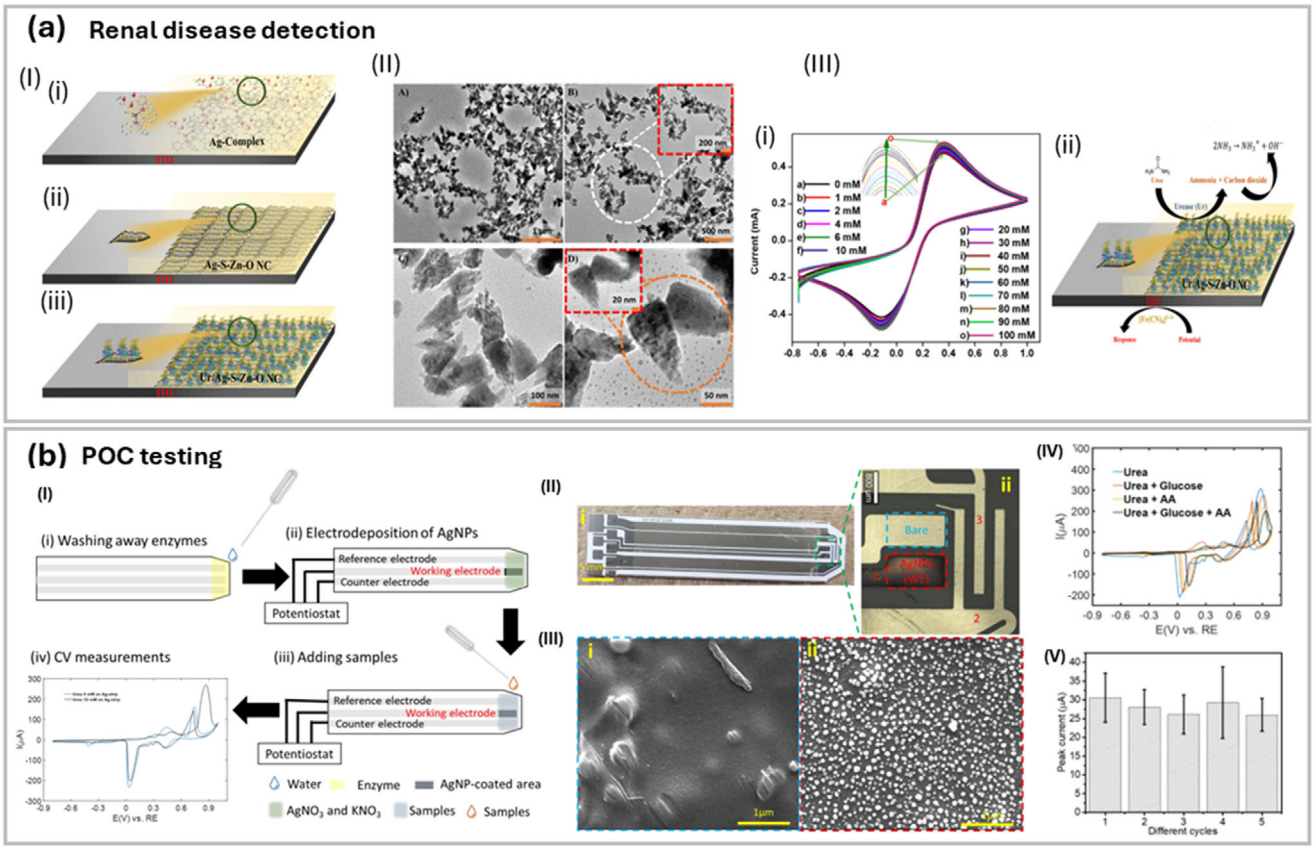

Figure 7. Nanoengineered Electrodes and Test Strip Development for Urea Detection: a-I) Nanoengineered Ag-S-Zn-O Electrodes for Urea Biosensing: (i) Hydrolyzed ITO glass substrate used for fabricating Ag complex electrodes (ii) Nanoengineered Ag-S-Zn-O electrodes (iii) Urease enzyme immobilized on the nanoengineered electrode interface. II) TEM images of the nanoengineered interface (III) Urea biosensor performance evaluation (i) urea biosensing performance for different concentrations ranging from 1 to 100 mM (ii) the sensing mechanism. Reproduced with permission.[183] Copyright 2024, ACS Publications. b) Electrochemical Test Strip for Urea Detection: I) Preparation steps of the test strip by removing the enzyme layer. Followed by electrodeposition of Ag nanoparticles on the test strip at −0.6 V (working versus reference electrode). This is followed by drop-casting of the sample onto the test strip for detection. II) Characterization of the fabricated test strip III) SEM images of Ag nanoparticle-coated strips. IV) Performance evaluation of the test strip in the presence of interfering substances. V) Performance stability across multiple test cycles. Reproduced with permission.[132] Copyright 2020, Nature.

concentration range in human blood, with a detection limit of 0.14 mM. The study also reported excellent selectivity, reproducibility, reusability, and storage stability for the modified test strips Figure 7b represents urea detection electrochemical test strip – fabrication steps, characterization, of Ag nanoparticle coating, performance evaluation with interferents, and stability over multiple cycles.[132] Kim et al. fabricated a portable biosensor for real-time monitoring of physiological fluids. Urease was immobilized on a polytetrafluoroethylene (PTFE) membrane using various linkers, and the membrane was placed within a PDMS fluidic chamber. Electrochemical signals were measured using chronoamperometry at a flow rate of 1 mL min^{-1}. The biosensor exhibited excellent repeatability and minimal interference, demonstrating its potential for monitoring urea concentrations in human patients.[187] Bose et al. proposed a single-use disposable paper-based sensor for the direct measurement of urea in whole blood samples. Their device employs impedimetric sensing technology with graphite electrodes, requiring only 0.2 mL of whole blood and providing results within 30 seconds. Compact and easy to use, this biosensor is ideal for home monitoring of urea levels.[188]

4.3. Other Clinical Significance

4.3.1. Diabetes Management

Serum urea and creatinine levels are widely recognized as essential markers for evaluating kidney function in individuals with diabetes mellitus.[189] Research suggests that elevated urea levels may exacerbate insulin resistance and impair insulin secretion.[180] While urea biosensors are not directly used for diabetes detection, a strong correlation exists between elevated urea levels, kidney dysfunction, and diabetes. Consequently, monitoring urea levels could provide preliminary insights into diabetes risk and related complications.[190–193]

4.3.2. Cancer Diagnostics

Chronic liver diseases (CLDs) present a global health challenge, accounting for ≈2 million deaths annually,[194,195] Liver fibrosis, a common outcome of CLDs, is a critical precursor to cirrhosis and its associated complications, significantly impacting liver func-

tion and quality of life.[195] Elevated urea levels have been linked to adverse liver conditions.[196] Experimental research indicates that even in the early stages of CLDs, compromised urea synthesis correlates with hepatic fibrosis. Additionally, disruptions in the urea cycle have been associated with cancer development. Patients with CLDs and lower urea levels may experience more advanced disease stages and face a heightened risk of disease progression,[197–199] Studies have suggested the potential of urea as a biomarker for hepatocellular carcinoma,[200] though this remains an emerging area of research. Other investigations propose using urea as a biomarker for neoplasm progression,[201] and further studies confirm the correlation between altered urea levels and cancer prevalence.[202] Disruptions in the urea cycle are increasingly viewed as indicators of neoplasm, providing new directions for cancer diagnostics.[199,203,204]

4.4. Using Urea Biosensor for Other Purposes/ Applications

Antimicrobial resistance is a growing global concern due to the overuse of antibiotics, making bacterial infections increasingly challenging to treat. This has created a pressing need for rapid and reliable bacterial detection methods to guide appropriate antibiotic administration. Traditional methods, such as bacterial culture, often require 24–96 h of incubation, while molecular analysis demands sophisticated equipment, posing significant challenges for healthcare facilities with limited resources.[205,206] To address this issue, researchers have focused on developing customizable and cost-effective biosensors for pathogen detection. For example, Yao et al. designed a microfluidic impedance biosensor for detecting *E. coli* O157:H7. This biosensor incorporates immunomagnetic nanoparticles (MNPs) for bacterial separation, urease for signal amplification, and a microfluidic chip for impedance measurement. Streptavidin-modified MNPs conjugated with biotinylated polyclonal antibodies (PAbs) were used to isolate bacteria from the sample, forming MNP-bacteria complexes. Gold nanoparticles (GNPs) conjugated with urease and specific aptamers were added, resulting in MNP-bacteria-GNPs-urease complexes. These complexes hydrolyze urea into ammonium carbonate, leading to a decrease in impedance. The study demonstrated a strong linear relationship between impedance change and *E. coli* concentration, achieving a low detection limit of 12 CFU m^{-1}.[207] A similar approach was employed by Wang et al. for detecting *Listeria monocytogenes*.[208] Additionally, Tzianni et al. developed a low-cost medical diagnostic device featuring a free-standing, pH-responsive membrane. This device offers a time-based signal output that reduces costs and simplifies usability, making it accessible to non-trained personnel. The biosensor, made from inexpensive materials, demonstrates excellent selectivity, tunable detection ranges, and adaptability for various biochemical indices and qualitative tests, such as detecting *H. pylori* in biopsy samples.[209]

5. Conclusion and Future Perspectives

Urea, a nitrogenous organic compound excreted in urine as a byproduct of protein metabolism, plays a critical role in clinical diagnostics. Maintaining optimal urea levels in blood and urine is vital, as elevated levels can indicate serious health conditions such as kidney disease or liver failure. Continuous monitoring of urea levels is particularly essential for patients with metabolic disorders to prevent complications. Despite significant advancements in urea detection over the years, traditional methods are still predominantly used in hospital settings. These techniques, while highly sensitive and specific, are often expensive, require skilled operators, are time-intensive, and are invasive. Recent research has focused on developing innovative materials, particularly nanomaterials, to address these limitations.

This review explored three primary approaches for urea detection: enzymatic amperometric, enzymatic potentiometric, and non-enzymatic methods. Enzymatic techniques, recognized for their high selectivity, directly detect urea but face challenges related to enzyme immobilization, stability, and cost. Non-enzymatic approaches, often employing cyclic voltammetry, offer improved stability and cost-effectiveness. Advancements in sensitivity, selectivity, and miniaturization have enhanced these biosensors for point-of-care applications. Additionally, strategies to improve long-term stability further support their potential in medical diagnostics, particularly for kidney function assessment and chronic disease management.

Electrochemical approaches have also leveraged advanced materials to enhance electron transfer efficiency. Materials like graphene-based compounds and metal oxides demonstrate exceptional sensitivity, low detection limits, and fast response times. Surprisingly, non-enzymatic methods, which do not directly detect urea, have shown remarkable performance, with metal oxide-based sensors outperforming enzymatic counterparts in terms of robustness, affordability, and sensitivity. Composite materials combining metal oxides, graphene derivatives, and conductive polymers hold great potential for next-generation urea biosensors. However, inconsistencies in reporting study parameters across the literature make it challenging to draw definitive conclusions. **Figure 8** presents three scatter plots, each highlighting a key performance characteristic, limit of detection (LOD), response time, and sensitivity of various materials used in enzymatic and non-enzymatic urea sensors. Each data point represents a specific material, with the x-axis categorizing materials based on their application in enzymatic or non-enzymatic sensors. This visualization facilitates a comparative analysis of material performance across different sensor types.

Based on the presented plots enzymatic materials consistently display lower LODs (better detection limits), often under 50 μM, compared to non-enzymatic materials, where several values exceed 400 μM. Carbon nanotube and rGO-based enzymatic sensors showed especially low LOD. In contrast, non-enzymatic candidates (e.g., nickel cobalt oxide nanoneedles, NiO-molybdenum trioxide) had much higher LODs, indicating less sensitivity at low analyte concentrations. Notably, a few non-enzymatic systems had very rapid response time, with some matching or outperforming enzymatic materials (e.g., Ag/NiO or copper-based), but the overall trend still favors enzymatic systems for rapid detection. On the other hand, non-enzymatic materials exhibit significantly higher sensitivities (often >1000 μA mM^{-1}), where enzymatic materials typically cluster below 100 μA mM^{-1}, with the exception of some platinum and rGO systems, but on average present notably lower sensitivity compared to the non-enzymatic group.

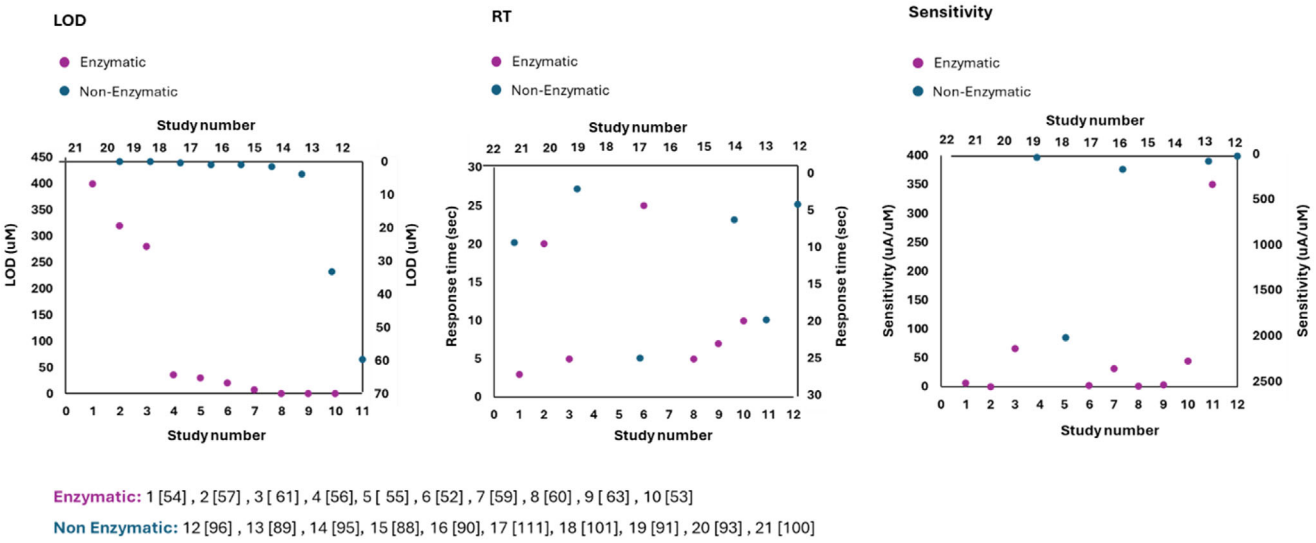

Figure 8. Comparative Analysis of Urea Biosensors Based on Detection Limit, Response Time, and Sensitivity: These scatter plots present a comparative analysis of various urea biosensors, differentiating between enzymatic and non-enzymatic approaches. The graph highlights key performance metrics, including the detection limit, response time, and sensitivity of different material compositions.

Notable best performers: Carbon nanotube and rGO-based enzymatic sensors showed especially low LOD. In contrast, non-enzymatic candidates (e.g., nickel cobalt oxide nanoneedles, NiO-molybdenum trioxide) had much higher LODs, indicating less sensitivity at low analyte concentrations.

While recent advances in enzymatic and non-enzymatic urea biosensors have demonstrated impressive sensitivity, response time, and stability, there remains significant scope for optimization to meet practical clinical and point-of-care demands. Based on the current state of the art, we recommend the following strategic directions to further enhance urea biosensor performance:

1) Material Engineering for Synergistic Effects: Future designs should focus on hybrid composite materials that combine the catalytic activity of metal oxides (such as NiO, CuO) with the exceptional electron transfer properties of carbon-based nanomaterials (e.g., graphene, carbon nanotubes). Such synergies can simultaneously lower detection limits and boost sensitivity while improving electrochemical stability.
2) Enzyme Immobilization and Stability Enhancement: For enzymatic biosensors, improving robustness and lifetime of immobilized urease remains critical. Employing novel cross-linking chemistries or encapsulation within biocompatible nanostructured matrices (e.g., hydrogels, polymeric nanoparticles) can protect enzyme activity against environmental stressors and minimize denaturation while maintaining rapid substrate accessibility. A robust biosensor should ensure stability and durability of the immobilized enzyme over time while maintaining consistent performance.[47] For industrial scale-up, a minimum operational stability of 1–3 months is typically advised for enzyme-based biosensors to guarantee constant performance and commercial feasibility.[210]
3) Minimizing Signal Noise through Advanced Electrode Design: Enhancing signal-to-noise ratio by optimizing electrode surface morphology to increase effective surface area and reduce fouling can improve detection reliability. Micro- and nano-patterned electrode architectures such as microneedle arrays show promise in achieving high signal fidelity in complex biological fluids.

Electrode selection: The working electrode, where electrochemical reactions occur, must exhibit a high signal-to-noise ratio, consistent response, stability, and low interference. Noble metals such as gold (Au), silver (Ag), platinum (Pt), and mercury (Hg), as well as carbon-based materials like carbon paste and graphite, are commonly used. Conductive polymers are also applied to enhance electron transfer.[211]

1) Non-Enzymatic Sensor Development for Cost-Effectiveness and Stability: Continued development of enzyme-free sensors leveraging metal-organic frameworks, doped metal oxides, and novel nanostructured catalysts can address issues of enzyme instability and reduce sensor cost. Tailoring nanomaterial morphology and doping elements can tune catalytic sites for selective and rapid urea oxidation.
2) Integration with Advanced Electronics and Artificial Intelligence: Coupling biosensors with miniaturized electronics, IoT-enabled platforms, and AI-based data analytics can facilitate real-time monitoring, enhanced data interpretation, and personalized health feedback. This integration is essential for translating sensor innovations into accessible, user-friendly clinical devices.
3) Standardization and Uniform Reporting: To accelerate progress, the community should adopt standardized protocols for biosensor characterization, including uniform metrics for sensitivity, LOD, stability, and reproducibility. Transparent reporting enables more meaningful cross-comparison and rational material and design selection.
4) Focus on Real-World Conditions and Sample Matrices: Biosensors should be rigorously evaluated in relevant biological fluids such as blood, urine, and sweat under dynamic

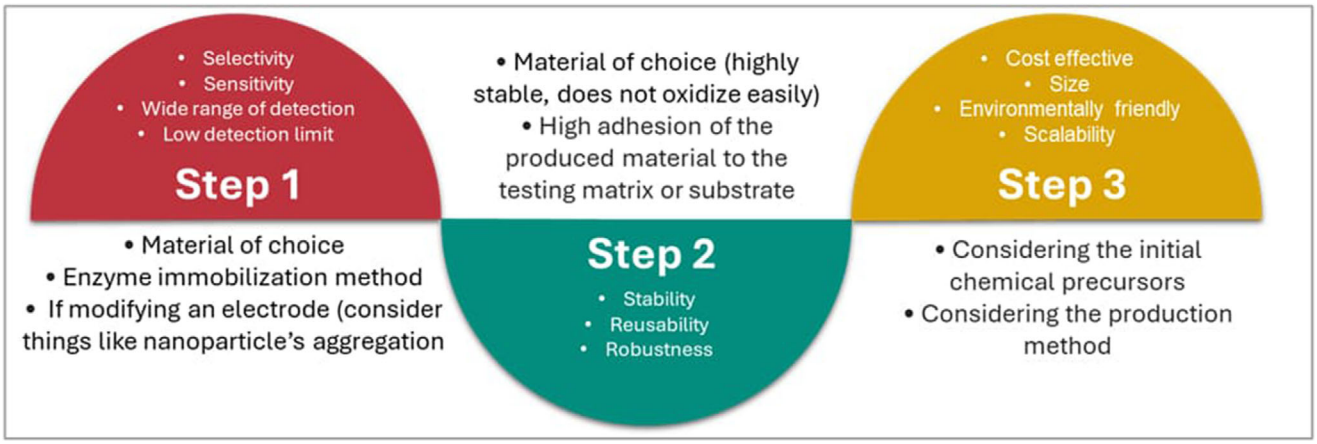

Figure 9. Summary of different parameters to consider when designing a urea biosensor: Step 1 Performance Considerations. This initial phase focuses on desired performance characteristics, including high selectivity and sensitivity, a wide range of detection, and a low detection limit. It also involves choosing appropriate materials, selecting an effective enzyme immobilization method, and addressing potential issues like nanoparticle aggregation when modifying an electrode. Step 2: Material and Operational Characteristics. This step emphasizes the material's qualities and operational functionality. This step concentrates on selecting a stable material that resists oxidation and has high adhesion to the testing matrix. Additionally, the focus includes ensuring the sensor's stability, reusability, and robustness. Step 3: Economic and Practical Considerations. This final phase considers the practical aspects of production and implementation, such as cost-effectiveness, size, environmental friendliness, and scalability. It also involves considering the initial chemical precursors and the production method to optimize the overall process.

physiological conditions to ensure stability, selectivity, and minimal interference. This would bring devices closer to clinical and at-home applicability.

In summary, by converging innovative material science with robust bioengineering techniques and smart system integration, next-generation urea biosensors can achieve superior analytical performance, cost-effectiveness, and practical deployment for continuous patient monitoring and early diagnostics. Our perspective encourages a multidisciplinary approach focused on both fundamental enhancements and translational readiness to maximize clinical impact.

Designing efficient urea biosensors requires careful consideration of factors such as selectivity, sensitivity, signal strength, noise levels, robustness, and ease of deployment. A high-performing biosensor should also be cost-effective, stable, sensitive, and reproducible. The below section briefly discusses a few aspects to consider when designing urea biosensor systems. **Figure 9** represents an overall flow of different parameters in consideration for successful urea detection.

Conflict of Interest

The authors declare no conflict of interest.

Keywords

amperometric sensing, electrochemical biosensors, enzymatic sensors, non-enzymatic sensors, potentiometric sensing, urea detection, urease-based sensors, wearable biosensors

Received: September 4, 2025
Published online:

[1] S. Singh, M. Sharma, G. Singh, *IET Nanobiotechnol.* **2021**, *15*, 358.
[2] S. N. Botewad, D. K. Gaikwad, N. B. Girhe, H. N. Thorat, P. P. Pawar, *Biotechnol. Appl. Biochem.* **2025**, *70*, 485.
[3] C. S. Pundir, S. Jakhar, V. Narwal, *Biosens. Bioelectron.*, **2019**, *123*, 36.
[4] M. F. Katta, S. Zemaitis, *Uremia- StatPearls-NCBI Bookshelf*, NCBI-StatPearls, Tampa, USA **2023**.
[5] A. Hosten, in *Clinical Methods: The History, Physical, and Laboratory Examinations*, 3rd ed., (Ed: H. K. Walker), Butterworths, Boston **1990**, ch. 193.
[6] V. Gounden, H. Bhatt, I. Jialal, *Renal Function Tests*, StatPearls Publishing, Treasure Island (FL) **2024**.
[7] E. Hamza, L. Metzinger, V. Metzinger-Le Meuth, *Cells*, **2020**, *9*, 2039.
[8] M. Liu, M. Li, J. Liu, H. Wang, D. Zhong, H. Zhou, B. Yang, *J. Transl. Med.* **2016**, *14*, 53.
[9] L. Quadrini, S. Laschi, C. Ciccone, F. Catelani, I. Palchetti, *TrAC, Trends Anal. Chem.* **2023**, *168*, 117345.
[10] C. P. Kovesdy, *Epidemiology of Chronic Kidney Disease: An Update 2022*, Elsevier B.V., Amsterdam **2022**.
[11] J. Sundstrom, J. Bodegard, A. Bollmann, M. G. Vervloet, P. B. Mark, A. Karasik, T. Taveira-Gomes, M. Botana, K. I. Birkeland, M. Thuresson, L. Jäger, M. M. Sood, G. VanPottelbergh, N. Tangri, C. C. Investigators, *Lancet Reg. Health* **2022**, *20*, 100447.
[12] C. for Disease Control, Chronic Kidney Disease in the United States, https://www.cdc.gov/kidneydisease/publications-resources/CKD-national-facts.html (accessed: September 2023).
[13] Z. A. Massy, C. Pietrement, F. Touré, *Semin Dial.* **2016**, *29*, 333.
[14] I. D. Federation, About diabetes- Facts and figures, https://idf.org/about-diabetes/diabetes-facts-figures/ (accessed: March 2024).
[15] National institute of diabetes and digestive and kindey diseases, High Blood Pressure and Kidney Disease, https://www.niddk.nih.gov/health-information/kidney-disease/high-blood-pressure (accessed: March 2024).
[16] O. Adeyomoye, C. Akintayo, K. Omotuyi, A. Adewumi, *Indian J. Nephrol.* **2022**, *32*, 539.

[17] M. H. Rosner, T. Reis, F. Husain-Syed, R. Vanholder, C. Hutchison, P. Stenvinkel, P. J. Blankestijn, M. Cozzolino, L. Juillard, K. Kashani, M. Kaushik, H. Kawanishi, Z. Massy, T. L. Sirich, L. Zuo, C. Ronco, *Clin. J. Am. Soc. Nephrol.* **2021**, *16*, 1918.
[18] E. P. Rhee, E. Guallar, S. Hwang, N. Kim, M. Tonelli, S. M. Moe, J. Himmelfarb, R. I. Thadhani, N. R. Powe, T. Shafi, *Kidney360* **2020**, *1*, 86.
[19] M. Mohamedali, S. Reddy Maddika, A. Vyas, V. Iyer, P. Cheriyath, *Int. J. Nephrol.* **2014**, *2014*, 520281.
[20] H. Lin, G. L.-H. Wong, X. Zhang, T. C.-F. Yip, K. Liu, Y. K. Tse, V. W.-K. Hui, J. C.-T. Lai, H. L.-Y. Chan, V. W.-S. Wong, *Clin. Mol. Hepatol.* **2022**, *28*, 77.
[21] Y. Gao, J. Jia, X. Liu, S. Guo, L. Ming, *Lab Med.* **2021**, *52*, 267.
[22] H. Shintani, *J. Liquid Chromatogr.* **1994**, *18*, 2167.
[23] M. Tabata, T. Murachi, *J. Biolumin. Chemilumin.* **1988**, *2*, 63.
[24] S. B. Barker, *J. Biol. Chem.* **1944**, *152*, 453.
[25] J. Bojic, B. Radovanovic, J. Dimitrijevic, *Anal. Sci.* **2008**, *24*, 769.
[26] T. Yuan, O. Voznyy, *Cell Rep. Phys. Sci.* **2023**, *4*, 101521.
[27] E. Safitri, L. Y. Heng, M. Ahmad, T. L. Ling, *Sens Actuators B Chem.* **2017**, *240*, 763.
[28] C. Y. Wu, Y. T. Su, C. K. Su, *Biosens. Bioelectron.* **2023**, *237*, 115500.
[29] S. Sharma, S. K. Mishra, *Chemosensors* **2023**, *11*, 421.
[30] I. T. Degim, S. Ilbasmis, R. Dundaroz, Y. Oguz, *Pediatr. Nephrol.* **2003**, *18*, 1032.
[31] J.-C. Chou, C.-Y. Wu, S.-H. Lin, P.-Y. Kuo, C.-H. Lai, Y.-H. Nien, Y.-X. Wu, T.-Y. Lai, *Sensors (Switzerland)* **2019**, *19*, 3004.
[32] M. A. Barahona Montero, A. C. Carmona Segnini, G. Salazar Álvarez, J. P. Pan Sanabria, *Economía y Sociedad* **2015**, *20*.
[33] S. Singh, M. Sharma, G. Singh, *IET Nanobiotechnol.* **2021**, *15*, 358.
[34] D. Pandya, A. K. Nagrajappa, K. S. Ravi, *J. Clin. Diagn. Res.* **2016**, *10*, ZC58.
[35] S. N. Botewad, D. K. Gaikwad, N. B. Girhe, H. N. Thorat, P. P. Pawar, *Biotechnol. Appl. Biochem.* **2021**, *70*, 485S.
[36] S. Singh, M. Sharma, G. Singh, *IET Nanobiotechnol.* **2021**, *15*, 358S.
[37] O. Özbek, C. Berkel, Ö. Isildak, I. Isildak, *Clin. Chim. Acta* **2022**, *524*, 154.
[38] F. Mashhadban-K, L. Gorgani, G. Najafpour-Darzi, *Sens. Actuators, A* **2024**, *374*, 115499.
[39] F. Shalileh, H. Sabahi, M. Dadmehr, M. Hosseini, *Microchem. J.* **2023**, *193*, 108990.
[40] R. Nagraik, A. Sharma, D. Kumar, P. Chawla, A. P. Kumar, *Sens. Biosens. Res.* **2021**, *33*, 100433.
[41] S. Venkatachalapathi, R. Shankararajan, K. Ramany, *Sens. Rev.* **2024**, *44*, 505.
[42] S. B. Adeloju, in *Encyclopedia of Analytical Science*, Elsevier Inc., United States **2005**, p 70.
[43] S. M. U. Ali, Z. H. Ibupoto, S. Salman, O. Nur, M. Willander, B. Danielsson, *Sens. Actuators, B* **2011**, *160*, 637.
[44] M. Alqasaimeh, L. Y. Heng, M. Ahmad, A. S. Santhana Raj, T. L. Ling, *Sensors (Switzerland)* **2014**, *14*, 13186.
[45] J. Erfkamp, M. Guenther, G. Gerlach, *Sensors (Switzerland)* **2019**, *19*, 2858.
[46] D. Fapyane, D. Berillo, J.-L. Marty, N. P. Revsbech, *ACS Omega* **2020**, *5*, 27582.
[47] H. H. Nguyen, S. H. Lee, U. J. Lee, C. D. Fermin, M. Kim, *Materials* **2019**, *12*, 121.
[48] J. Razumiene, V. Gureviciene, I. Sakinyte, L. Rimsevicius, V. Laurinavicius, *Sensors* **2020**, *20*, 4496.
[49] S. Selvarajan, A. Suganthi, M. Rajarajan, *Ultrason. Sonochem.* **2018**, *42*, 183.
[50] J. Razumiene, V. Gureviciene, I. Sakinyte, L. Rimsevicius, V. Laurinavicius, *Sensors (Switzerland)* **2020**, *20*, 4496.
[51] R. Y. A. Hassan, A. M. Kamel, M. S. Hashem, H. N. A. Hassan, M. A. Abd El-Ghaffar, *J. Solid State Electrochem.* **2018**, *22*, 1817.
[52] R. M. Apetrei, N. Guven, P. Camurlu, *ChemistrySelect* **2024**, *9*, e202303424.
[53] S. Korkut, S. Uzuncar, M. S. Kilic, B. Hazer, *Instrum. Sci. Technol.* **2019**, *47*, 1.
[54] A. Prabakaran, B. S. Hameed, K. S. S. Devi, U. M. Krishnan, *Chem. Pap.* **2023**, *77*, 4265.
[55] D. Wang, X. Mao, Y. Liang, Y. Cai, T. Tu, S. Zhang, T. Li, L. Fang, Y. Zhou, Z. Wang, Y. Jiang, X. Ye, B. Liang, *Biosensors (Basel)* **2023**, *13*, 272.
[56] S. Korkut Uru, M. S. Kilic, F. Yetiren, *Electroanalysis* **2021**, *33*, 1911.
[57] M. Hosseinian, G. Najafpour, A. Rahimpour, *Turk. J. Chem.* **2019**, *43*, 1063.
[58] M. Tyagi, M. Tomar, V. Gupta, *Mater. Sci. Eng., B* **2019**, *240*, 147.
[59] M. Mikani, R. Rahmanian, *J. Anal. Chem.* **2021**, *76*, 981.
[60] E. Muthusankar, V. K. Ponnusamy, D. Ragupathy, *Synth. Met.* **2019**, *254*, 134.
[61] S. Evli, U. Kilimci, M. Karagöz, M. Uygun, D. Aktaş Uygun, *Microchem. J.* **2024**, *200*, 110500.
[62] S. Sharma, R. Sain, S. Yadav, M. Sharma, *Microchem. J.* **2024**, *205*, 111415.
[63] T. Çamurcu, V. Sanko, İ. Ömeroğlu, S. O. Tümay, A. Şenocak, *Anal. Methods* **2024**, *16*, 6696.
[64] S. Uzunçar, L. Meng, A. P. F. Turner, W. C. Mak, *Biosens. Bioelectron.* **2021**, *171*, 112725.
[65] K. C. Honeychurch, in *Printed Films: Materials Science and Applications in Sensors, Electronics and Photonics*, Elsevier Ltd., Amsterdam **2012**, pp. 366–409.
[66] J. Wang, *Analytical Electrochemistry*, 3rd ed., John Wiley & Sons, Inc, Hoboken, NJ **2006**.
[67] M. Mascini, G. G. Guilbault, *Biosensors (Basel)* **1986**, *2*, 147.
[68] M. Urbanowicz, K. Sadowska, A. Paziewska-Nowak, A. Sołdatowska, D. G. Pijanowska, *Membranes (Basel)* **2021**, *11*, 898.
[69] N. L. Walker, A. B. Roshkolaeva, A. I. Chapoval, J. E. Dick, *Curr. Opin. Electrochem.* **2021**, *28*, 100735.
[70] O. Özbek, C. Berkel, Ö Isildak, I. Isildak, *Clin. Chim. Acta* **2022**, *524*, 154.
[71] W. Prissanaroon-Ouajai, A. Sirivat, P. J. Pigram, N. Brack, *Macromol. Symp.* **2015**, *354*, 334.
[72] D. Chirizzi, C. Malitesta, *Sens. Actuators, B* **2011**, *157*, 211.
[73] B. Lakard, D. Magnin, O. Deschaume, G. Vanlancker, K. Glinel, S. Demoustier-Champagne, B. Nysten, A. M. Jonas, P. Bertrand, S. Yunus, *Biosens. Bioelectron.* **2011**, *26*, 4139.
[74] C. Y. (Kevin) Lai, P. J. S. Foot, J. W. Brown, P. Spearman, *Biosensors (Basel)* **2017**, *7*, 13.
[75] H. J. N. P. D. Mello, M. Mulato, *Biomed. Microdevices* **2020**, *22*, 22.
[76] C. S. Kushwaha, P. Singh, N. S. Abbas, S. K. Shukla, *J. Mater. Sci.: Mater. Electron.* **2020**, *31*, 11887.
[77] W. Prissanaroon-Ouajai, A. Sirivat, *Key Eng. Mater.* **2020**, *856*, 286.
[78] M. Guzinski, J. M. Jarvis, P. D'Orazio, A. Izadyar, B. D. Pendley, E. Lindner, *Anal. Chem.* **2017**, *89*, 8468.
[79] B. Öndeş, F. Akpınar, M. Uygun, M. Muti, D. Aktaş Uygun, *Microchem. J.* **2021**, *160*, 105667.
[80] M. Situmorang, P. Kaban, R. Ayulinova, W. Hutabarat, presented at Proceedings of The 5th Annual International Seminar on Trends in Science and Science Education, AISTSSE 2018, Medan, Indonesia, October **2019**.
[81] Y.-H. Nien, T.-Y. Su, J.-C. Chou, C.-H. Lai, P.-Y. Kuo, S.-H. Lin, T.-Y. Lai, M. Rangasamy, *IEEE Trans. Instrum. Meas.* **2021**, *70*, 1500409.
[82] A. Bonini, F. M. Vivaldi, E. Herrera, B. Melai, A. Kirchhain, N. V. P. Sajama, M. Mattonai, R. Caprioli, T. Lomonaco, F. D. Francesco, P. Salvo, *IEEE Sens. J.* **2020**, *20*, 4571.
[83] S. Jakhar, C. S. Pundir, *Biosens. Bioelectron.* **2018**, *100*, 242.
[84] F. Wang, F. Zhang, Q. Wang, P. He, *Anal. Chem.* **2022**, *94*, 14434.

[85] J.-C. Chou, C.-Y. Wu, P.-Y. Kuo, C.-H. Lai, Y.-H. Nien, Y.-X. Wu, S.-H. Lin, Y.-H. Liao, *IEEE Trans. Nanotechnol.* **2019**, *18*, 484.
[86] Y.-H. Nien, T.-Y. Su, C.-S. Ho, J.-C. Chou, C.-H. Lai, P.-Y. Kuo, Z.-X. Kang, Z.-X. Dong, T.-Y. Lai, C.-H. Wang, *IEEE Trans. Electron Devices* **2020**, *67*, 5104.
[87] J. P. Prajapati, P. Singh, K. R. Singh, J. Singh, S. Mallick, R. P. Singh, *J. Mol. Struct.* **2024**, *1307*, 137918.
[88] R. A. Alshgari, M. D. Albaqami, A. A. Shah, M. H. Ibupoto, S. Kumar, I. A. Halepoto, U. Aftab, A. Nafady, M. Willander, A. Tahira, Z. H. Ibupoto, *J. Mater. Sci.: Mater. Electron.* **2022**, *33*, 25250.
[89] S. Himori, T. Sakata, *Sens. Actuators, B* **2023**, *393*, 134239.
[90] A. Mohammadpour-Haratbar, S. Mohammadpour-Haratbar, Y. Zare, K. Y. Rhee, S. J. Park, *Biosensors* **2022**, *12*, 1004.
[91] H. Yamada, K. Yoshii, M. Asahi, M. Chiku, Y. Kitazumi, *Electrochemistry* **2022**, *90*, 102005.
[92] M. Junaid, Noor-ul-Ain, R. Jabeen, S. A. Buzdar, W. Qamar khan, M. Anwar, M. Javed, M. F. Warsi, *Phys. B Condens. Matter* **2023**, *651*, 414592.
[93] S. Amin, A. Tahira, A. Solangi, V. Beni, J. R. Morante, X. Liu, M. Falhman, R. Mazzaro, Z. H. Ibupoto, A. Vomiero, *RSC Adv.* **2019**, *9*, 14443.
[94] N. Salarizadeh, M. Habibi-Rezaei, S. J. Zargar, *Mater. Chem. Phys.* **2022**, *281*, 125870.
[95] S. Mangrio, A. Tahira, I. A. Mahar, M. Parveen, A. A. Hullio, D. A. Solangi, A. Khawaja, M. A. Bhatti, Z. A. Ibupoto, A. B. Mallah, A. Nafady, E. A. Dawi, A. Al Karim Haj Ismail, M. Emo, B. Vigolo, Z. H. Ibupoto, *J. Nanopart. Res.* **2023**, *25*, 195.
[96] A. D. Irzalinda, J. Gunlazuardi, R. Wibowo, *J. Phys.: Conf. Ser.* **2020**, *1442*, 012054.
[97] X. Wang, B. Liu, J. Li, Y. Zhai, H. Liu, L. Li, H. Wen, *Electroanalysis* **2021**, *33*, 1484.
[98] T. S. Sunil Kumar Naik, S. Saravanan, K. N. Sri Saravana, U. Pratiush, P. C. Ramamurthy, *Mater. Chem. Phys.* **2020**, *245*, 122798.
[99] S. Maleki Nia, F. Kheiri, E. Jannatdoust, M. Sirousazar, V. A. Chianeh, G. Kheiri, *J. Electrochem. Soc.* **2021**, *168*, 067504.
[100] Z. Zhao, J. Xiao, X. Zhang, J. Jiang, M. Zhang, Y. Li, T. Li, J. Wang, *Microchem. J.* **2023**, *190*, 108634.
[101] G. Abdollahi, M. H. Mashhadizadeh, *Russ. J. Electrochem.* **2024**, *60*, 571.
[102] S. Güngör, C. Taşaltın, İ. Gürol, G. Baytemir, S. Karakuş, N. Taşaltın, *Appl. Phys. A Mater. Sci. Process* **2022**, *128*, 89.
[103] H. S. Magar, R. Y. A. Hassan, M. N. Abbas, *Sci. Rep.* **2023**, *13*, 2034.
[104] P. Ray, S. Pal, A. Sarkar, F. Sultana, A. Basu, B. Show, *ACS Appl. Bio Mater.* **2024**, *7*, 1621.
[105] T. H. V. Kumar, A. K. Sundramoorthy, *J. Electrochem. Soc.* **2018**, *165*, B3006.
[106] J. Yoon, D. Lee, E. Lee, Y. S. Yoon, D. Kim, *Electroanalysis* **2019**, *31*, 17.
[107] S. Pal, D. Kumar, S. Pillay, S. K. Shukla, C. M. Hussain, *Top. Catal.* **2025**, https://doi.org/10.1007/s11244-025-02058-3.
[108] S. Khataee, G. Dehghan, Z. Shaghaghi, A. Khataee, *Microchim. Acta* **2024**, *191*, 152.
[109] M. Parveen, I. A. Mahar, A. Tahira, G. M. Thebo, A. A. Hulio, M. A. Bhatti, I. Naz, A. Z. Naqvi, A. A. Shah, E. Dawi, A. A. K. H. Ismail, M. A. Jakhrani, L. Saleem, A. Nafady, Z. H. Ibupoto, *Microchem. J.* **2024**, *204*, 111188.
[110] Z. Parsaee, *Ultrason. Sonochem.* **2018**, *44*, 120.
[111] N. Taşaltın, E. Aydın, S. Karakuş, A. Kilislioğlu, *Appl. Phys. A* **2020**, *126*, 827.
[112] S. Yadav, S. Kumar, N. Rani, S. Panwar, Poonam, Gauri, Chetan, S. Gupta, R. K. Choubey, S. Babu, V. Kumar, *J. Mater. Sci.: Mater. Electron.* **2024**, *35*, 1623.
[113] D. Ariyanti, D. Iswantini, N. Nurhidayat, H. Effendi, *Syst. Rev. Pharm.* **2020**, *11*, 1371.
[114] M. Morales-Cruz, N. E. Solis-Marcano, C. Binder, C. Priest, C. R. Cabrera, *Curr. Res. Biotechnol.* **2019**, *1*, 22.
[115] J. Shalini, K. J. Sankaran, C.-Y. Lee, N.-H. Tai, I.-N. Lin, *Biosens. Bioelectron.* **2014**, *56*, 64.
[116] H. Zhang, Y. Gan, S. Yang, K. Sheng, P. Wang, *Microsyst. Nanoeng.* **2021**, *7*, 51.
[117] G. Li, F. Xiao, S. Liao, Q. Chen, J. Zhou, Z. Wu, R. Yu, *Sens. Actuators, B* **2018**, *277*, 591.
[118] R. Ramesh, P. Puhazhendi, J. Kumar, M. K. Gowthaman, S. F. D'Souza, N. R. Kamini, *Mater. Sci. Eng., C* **2015**, *49*, 786.
[119] J. Mocaka, A. M. Bonda, S. Mitchella, G. Scollaryb, "international union of pure and applied chemistry analytical chemistry division commission on electroanalytical chemistry* a statistical overview of standard (iupac and acs) and new procedures for determining the limits of detection and quantification: application to voltammetric and stnpping techniques Prepared for publication by," **1997**.
[120] J. Liu, S. Wagan, M. Dávila Morris, J. Taylor, R. J. White, *Anal. Chem.* **2014**, *86*, 11417.
[121] N. Arroyo-Currás, K. Scida, K. L. Ploense, T. E. Kippin, K. W. Plaxco, *Anal. Chem.* **2017**, *89*, 12185.
[122] K. Fu, J.-W. Seo, V. Kesler, N. Maganzini, B. D. Wilson, M. Eisenstein, B. Murmann, H. T. Soh, *Adv. Sci.* **2021**, *8*, 2102495.
[123] L. Soleymani, Z. Fang, E. H. Sargent, S. O. Kelley, *Nat. Nanotechnol.* **2009**, *4*, 844.
[124] M. Senel, M. Dervisevic, N. H. Voelcker, *Mater. Lett.* **2019**, *243*, 50.
[125] V. Sanko, A. Şenocak, S. O. Tümay, E. Demirbas, *Bioelectrochemistry* **2023**, *149*, 108324.
[126] C. Bao, Q. Niu, Z. A. Chen, X. Cao, H. Wang, W. Lu, *RSC Adv.* **2019**, *9*, 29474.
[127] J. Yoon, Y. S. Yoon, D. J. Kim, *ACS Appl. Nano Mater.* **2020**, *3*, 7651.
[128] P. Arul, N. S. K. Gowthaman, S. A. John, S. T. Huang, *Mater. Chem. Front.* **2021**, *5*, 1942.
[129] J. Dunn, L. Kidzinski, R. Runge, D. Witt, J. L. Hicks, S. M. Schüssler-Fiorenza Rose, X. Li, A. Bahmani, S. L. Delp, T. Hastie, M. P. Snyder, *Nat. Med.* **2021**, *27*, 1105.
[130] A. A. Smith, R. Li, Z. T. H. Tse, *Sci. Rep.* **2023**, *13*, 4998.
[131] X. Pei, M. Sun, J. Wang, J. Bai, X. Bo, M. Zhou, *Small* **2022**, *18*, 2205061.
[132] J. Liu, R. Siavash Moakhar, A. Sudalaiyadum Perumal, H. N. Roman, S. Mahshid, S. Wachsmann-Hogiu, *Sci. Rep.* **2020**, *10*, 9527.
[133] Y.-L. Liu, R. Liu, Y. Qin, Q.-F. Qiu, Z. Chen, S.-B. Cheng, W.-H. Huang, *Anal. Chem.* **2018**, *90*, 13081.
[134] K. Kim, J. Lee, B. M. Moon, Y. B. Seo, C. H. Park, M. Park, G. Y. Sung, *Sensors* **2018**, *18*, 2607.
[135] P.-Y. Kuo, Z.-X. Dong, Y.-Y. Chen, *IEEE Trans. Instrum. Meas.* **2021**, *70*, 4004613.
[136] F. T. S. M. Ferreira, R. B. R. Mesquita, A. O. S. S. Rangel, *Microchem. J.* **2023**, *193*, 109102.
[137] P.-Y. Kuo, T.-H. Wang, M.-T. Hsu, C.-H. Liao, *IEEE J. Electron. Devices Soc.* **2023**, *11*, 337.
[138] M. D. Fernández-Ramos, M. Bolaños-Bañuelos, L. F. Capitán-Vallvey, *Talanta* **2023**, *254*, 124189.
[139] A. Soni, R. K. Surana, S. K. Jha, *Sens Actuators B Chem* **2018**, *269*, 346.
[140] G. Ibáñez-Redín, G. Rosso Cagnani, N. O. Gomes, P. A. Raymundo-Pereira, S. A. S. Machado, M. A. Gutierrez, J. E. Krieger, O. N. Oliveira, *Biosens. Bioelectron.* **2023**, *223*, 114994.
[141] S. Nur Ashakirin, M. Aniq Shazni, M. Hazani, M. M. Farhanulhakim Razipwee, E. Mahmoudi, *Measurement (Lond)* **2022**, *196*, 111058.
[142] J. Yoon, M. Sim, T.-S. Oh, Y. S. Yoon, D.-J. Kim, *J. Electrochem. Soc.* **2021**, *168*, 117510.
[143] D. Roy, P. Singh, S. Halder, N. Chanda, S. Mandal, *Bioelectrochemistry* **2021**, *142*, 107893.

[144] C. T. Nhu, P. N. Dang, T. B. Thanh, T. C. Duc, *Minist. Sci. Technol.* **2023**, *65*, 19.
[145] M. Dervisevic, M. J. Jara Fornerod, J. Harberts, P. S. Zangabad, N. H. Voelcker, *ACS Sens.* **2024**, *9*, 932.
[146] J. Mohebbi Najm Abad, A. Farahbakhsh, M. Mir, R. Alizadeh, A. Hekmatmanesh, *Sensors* **2023**, *23*, 8180.
[147] M. Zarei, *TrAC, Trends Anal. Chem.* **2017**, *91*, 26.
[148] X. Kou, L. Tong, Y. Shen, W. Zhu, L. Yin, S. Huang, F. Zhu, G. Chen, G. Ouyang, *Biosens. Bioelectron.* **2020**, *156*, 112095.
[149] H. Jiang, J. Yang, K. Wan, D. Jiang, C. Jin, *ACS Sens.* **2020**, *5*, 1325.
[150] Y. Bai, Q. Guo, J. Xiao, M. Zheng, D. Zhang, J. Yang, *Sens. Actuators, B* **2021**, *346*, 130447.
[151] M. Elsherif, M. U. Hassan, A. K. Yetisen, H. Butt, *ACS Nano* **2018**, *12*, 5452.
[152] A. Jędrzak, M. Kuznowicz, T. Rębiś, T. Jesionowski, *Bioelectrochemistry* **2022**, *145*, 108071.
[153] S. Liu, Z. Shen, L. Deng, G. Liu, *Biosens. Bioelectron.* **2022**, *209*, 114251.
[154] L. I. Tzianni, I. Moutsios, D. Moschovas, A. Avgeropoulos, K. Govaris, L. Panagiotidis, M. I. Prodromidis, *Biosens. Bioelectron.* **2022**, *207*, 114204.
[155] J. Cheng, J. Guo, X. Li, J. Guo, *Biosens. Bioelectron.* **2023**, *235*, 115410.
[156] K. Teekayupak, C. Aumnate, A. Lomae, P. Preechakasedkit, C. S. Henry, O. Chailapakul, N. Ruecha, *Talanta* **2023**, *254*, 124131.
[157] D. Ji, S. S. Low, D. Zhang, L. Liu, Y. Lu, Q. Liu, *Biomedical Engineering Technologies*, (Eds: M. R. Ossandon, H. Baker, A. Rasooly), *2393*, Humana, New York **2022**, p. 493.
[158] Z. Wu, P. Zhang, W. Xiao, Q. Chen, W. Lin, P. Chen, K. Chen, Q. Fu, Z. Wang, L. Zheng, *J. Pharm. Anal.* **2024**, *13*, 101041.
[159] J. Su, S. Chen, Y. Dou, Z. Zhao, X. Jia, X. Ding, S. Song, *Anal. Chem.* **2022**, *94*, 3235.
[160] C.-K. Choi, S. M. Shaban, B.-S. Moon, D.-G. Pyun, D.-H. Kim, *Anal. Chim. Acta* **2021**, *1170*, 338630.
[161] J. Cheng, Y. Fu, J. Guo, J. Guo, *Sens Actuators B Chem* **2023**, *387*, 133795.
[162] F. Shalileh, H. Sabahi, M. Golbashy, M. Dadmehr, M. Hosseini, *Anal. Chim. Acta* **2023**, *1284*, 341935.
[163] S. Jain, A. Paliwal, V. Gupta, M. Tomar, *Biosens. Bioelectron.* **2022**, *201*, 113919.
[164] J. Liu, X. Jiang, R. Zhang, Y. Zhang, L. Wu, W. Lu, J. Li, Y. Li, H. Zhang, *Adv. Funct. Mater.* **2019**, *29*, 1807326.
[165] H. J. Nogueira Pedroza Dias Mello, P. R. Bueno, M. Mulato, *Anal. Methods* **2020**, *12*, 4199.
[166] N. Larpant, A. D. Pham, A. Shafaat, J. F. Gonzalez-Martinez, J. Sotres, J. Sjöholm, W. Laiwattanapaisal, F. Faridbod, M. R. Ganjali, T. Arnebrant, T. Ruzgas, *Sci. Rep.* **2019**, *9*, 12948.
[167] P. Y. Kuo, T. H. Wang, M. T. Hsu, C. H. Liao, *IEEE Access* **2023**, *11*, 113694.
[168] S. N. Prabhu, C. P. Gooneratne, K.-A. Hoang, S. C. Mukhopadhyay, *IEEE Sens. J.* **2021**, *21*, 14320.
[169] D. Grieshaber, R. MacKenzie, J. Vörös, E. Reimhult, *Sensors* **2008**, *8*, 1400.
[170] R. Koncki, *Anal. Chim. Acta* **2007**, *599*, 7.
[171] N. P., J. Wekalao, A. N., S. K. Patel, *Plasmonics* **2024**, *20*, 2109.
[172] K. Su, G. Xiang, C. Cui, X. Jiang, Y. Sun, W. Zhao, L. He, *Arabian J. Chem.* **2023**, *16*, 104538.
[173] P. Y. Kuo, Z. X. Dong, Y. Y. Chen, *IEEE Trans. Nanotechnol.* **2021**, *20*, 311.
[174] Y.-H. Nien, T.-Y. Su, J.-C. Chou, P.-Y. Kuo, C.-H. Lai, C.-S. Ho, Z.-X. Dong, Z.-X. Kang, T.-Y. Lai, *IEEE J. Electron. Devices Soc.* **2021**, *9*, 242.
[175] T. K. Zeleke, L. K. Kemal, E. A. Mehari, F. D. Sema, A. M. Seid, G. A. Mekonnen, R. B. Abebe, *Heliyon* **2024**, *10*, e24618.
[176] L. A. Inker, C. H. Schmid, H. Tighiouart, J. H. Eckfeldt, H. I. Feldman, T. Greene, J. W. Kusek, J. Manzi, F. Van Lente, Y. L. Zhang, J. Coresh, A. S. Levey, *N. Engl. J. Med.* **2012**, *367*, 20.
[177] M. S. Younes-Ibrahim, M. Younes-Ibrahim, *J. Lab. Precis. Med.* **2022**, *7*, 20.
[178] J. H. Ix, M. G. Shlipak, *Am. J. Kidney Dis.* **2021**, *78*, 719.
[179] S. M. Laville, A. Couturier, O. Lambert, M. Metzger, N. Mansencal, C. Jacquelinet, M. Laville, L. Frimat, D. Fouque, C. Combe, B. M. Robinson, B. Stengel, S. Liabeuf, Z. A. Massy, C. Ayav, S. Briançon, D. Cannet, C. Combe, D. Fouque, L. Frimat, Y.-E. Herpe, C. Jacquelinet, M. Laville, Z. A. Massy, C. Pascal, B. M. Robinson, B. Stengel, C. Lange, K. Legrand, S. Liabeuf, et al., *Nephrol., Dial., Transplant.* **2023**, *38*, 184.
[180] E. M. Brookes, D. A. Power, *Sci. Rep.* **2022**, *12*, 20827.
[181] N. Yadav, J. Narang, A. K. Chhillar, J. S. Rana, M. U. Mohd Siddique, E.-R. Kenawy, S. Alkahtani, M. N. Ahsan, A. K. Nayak, M. S. Hasnain, *Sens. Int.* **2024**, *5*, 100253.
[182] D. R. N. Zusfahair, E. D. P. Lestari, A. Fatoni, *Molekul* **2019**, *14*, 64.
[183] K. Kumar, K. R. Singh, R. S. Rathour, J. Singh, S. Bhattacharya, S. S. Pandey, *Langmuir* **2024**, *40*, 21052.
[184] C. P. Price, *BMJ* **2001**, *322*, 1285.
[185] D. Bhatia, S. Paul, T. Acharjee, S. S. Ramachairy, *Sens. Int.* **2024**, *5*, 100257.
[186] M. Berto, C. Diacci, L. Theuer, M. Di Lauro, D. T. Simon, M. Berggren, F. Biscarini, V. Beni, C. A. Bortolotti, *Flex. Print. Electron.* **2018**, *3*, 024001.
[187] J. Kim, G. Y. Sung, M. Park, *Biomedicines* **2020**, *8*, 596.
[188] A. Bose, K. Biswas, *IEEE Sens. J.* **2022**, *22*, 17275.
[189] A. Anwar, F. Faisal, W. Elahi, A. Illahi, S. M. Alam, S. T. A. Adnan, S. A. Batool, S. Bhagwandas, A. A. Hashmi, *Cureus* **2024**, *16*, e57022.
[190] J.-B. Zhong, Y.-F. Yao, G.-Q. Zeng, Y. Zhang, B.-K. Ye, X.-Y. Dou, L. Cai, *Sci. Rep.* **2023**, *13*, 9881.
[191] J. Du, W. Zhang, J. Niu, S. Wang, *Front. Endocrinol. (Lausanne)* **2024**, *15*, 1282015.
[192] Y. Xie, B. Bowe, T. Li, H. Xian, Y. Yan, Z. Al-Aly, *Kidney Int.* **2018**, *93*, 741.
[193] J.-B. Zhong, Y.-F. Yao, G.-Q. Zeng, Y. Zhang, B.-K. Ye, X.-Y. Dou, L. Cai, *Sci. Rep.* **2023**, *13*, 9881.
[194] Z. M. Younossi, M. Stepanova, Y. Younossi, P. Golabi, A. Mishra, N. Rafiq, L. Henry, *Gut* **2020**, *69*, 564.
[195] V. W.-S. Wong, L. A. Adams, V. de Lédinghen, G. L.-H. Wong, S. Sookoian, *Nat. Rev. Gastroenterol. Hepatol.* **2018**, *15*, 461.
[196] K. L. Thomsen, H. Grønbæk, E. Glavind, L. Hebbard, N. Jessen, A. Clouston, J. George, H. Vilstrup, *Am. J. Physiol.-Gastrointest. Liver Physiol.* **2014**, *307*, G295.
[197] F. De Chiara, S. Heebøll, G. Marrone, C. Montoliu, S. Hamilton-Dutoit, A. Ferrandez, F. Andreola, K. Rombouts, H. Grønbæk, V. Felipo, J. Gracia-Sancho, R. P. Mookerjee, H. Vilstrup, R. Jalan, K. L. Thomsen, *J. Hepatol.* **2018**, *69*, 905.
[198] F. De Chiara, K. L. Thomsen, A. Habtesion, H. Jones, N. Davies, J. Gracia-Sancho, N. Manicardi, A. Hall, F. Andreola, H. L. Paish, L. H. Reed, A. A. Watson, J. Leslie, F. Oakley, K. Rombouts, R. P. Mookerjee, J. Mann, R. Jalan, *Hepatology* **2020**, *71*, 874.
[199] J. S. Lee, L. Adler, H. Karathia, N. Carmel, S. Rabinovich, N. Auslander, R. Keshet, N. Stettner, A. Silberman, L. Agemy, D. Helbling, R. Eilam, Q. Sun, A. Brandis, S. Malitsky, M. Itkin, H. Weiss, S. Pinto, S. Kalaora, R. Levy, E. Barnea, A. Admon, D. Dimmock, N. Stern-Ginossar, A. Scherz, S. C. S. Nagamani, M. Unda, D. M. Wilson, R. Elhasid, A. Carracedo, et al., *Cell* **2018**, *174*, 1559.
[200] C. Bai, H. Wang, D. Dong, T. Li, Z. Yu, J. Guo, W. Zhou, D. Li, R. Yan, L. Wang, Z. Wang, Y. Li, L. Ren, *Front. Cell Dev. Biol.* **2021**, *9*, 650748.

[201] L. M. Obukhova, E. I. Erlykina, I. A. Medyanik, A. S. Grishin, A. M. Shutova, *J. Biosci. Med. (Irvine)* **2024**, *12*, 650748.
[202] C. Wang, H. Sun, J. Liu, *Eur. J. Med. Res.* **2023**, *28*, 213.
[203] N. Ghosh, S. Mahalanobish, P. C. Sil, *Biochem. Pharmacol.* **2024**, *228*, 116326.
[204] G. Lucarelli, M. Ferro, P. Ditonno, M. Battaglia, *Transl. Cancer Res.* **2018**, *7*, S766.
[205] C. Llor, L. Bjerrum, *Ther. Adv. Drug Saf.* **2014**, *5*, 229.
[206] E. Cesewski, B. N. Johnson, *Biosens. Bioelectron.* **2020**, *159*, 112214.
[207] L. Yao, L. Wang, F. Huang, G. Cai, X. Xi, J. Lin, *Sens. Actuators, B* **2018**, *259*, 1013.
[208] D. Wang, Q. Chen, H. Huo, S. Bai, G. Cai, W. Lai, J. Lin, *Food Control* **2017**, *73*, 555.
[209] E. I. Tzianni, J. Hrbac, D. K. Christodoulou, M. I. Prodromidis, *Sens. Actuators, B* **2020**, *304*, 127356.
[210] J. I. Reyes-De-Corcuera, H. E. Olstad, R. García-Torres, *Annu. Rev. Food Sci. Technol.* **2018**, *9*, 293.
[211] C. C. Liu, *Biosensors* **2012**, *2*, 269.

Samar Shurbaji is currently a PhD student at Qatar University (QU). She received her B.Sc. in biomedical sciences in 2016 and pursued her master's degree in materials science and technology, which she completed in 2019, both from Qatar University. MS. Shurbaji's experience is heavily focused on projects related to the biomaterials and microfluidics fields. She was involved in diverse projects including nanomaterials production, materials fabrication, and inducing shear stress over a cell's monolayer using microfluidic devices. She also previously contributed to research at the Hamad Bin Khalifa University (HBKU) on an integrated bioluminescence sensing system.

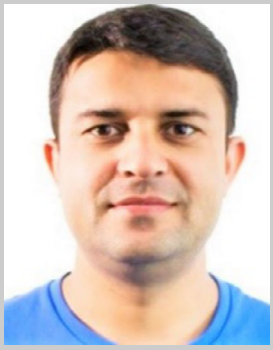

Arshad Khan holds a Ph.D. in Mechanical Engineering from the University of Hong Kong and a Master's degree in Mechatronic Engineering from Jeju National University. He is currently a research fellow at the Hamad Bin Khalifa University, Qatar Foundation. His prior experiences include a joint postdoctoral research fellowship at the Max Planck Institute for Informatics (MPI-Inf) and the Leibniz Institute for New Materials (Leibniz-INM) and lectureship at G.I.K Institute of Engineering Sciences and Technology. Dr. Khan's current research focuses on advancing self-powered, soft wearable electronics tailored for human activities and health monitoring.

Mohammad K. Hassan is an associate professor at the Center for Advanced Materials, Qatar University. His research interests include membranes development and characterization, polymer composites, and biodegradable polymers. He has published three patent and more than 120 articles in internationally renowned journals. His publications received more than 4427 citations with h-index of 39, according to Google Scholar. His research has been funded with more than $6 M from the Qatar National Research Fund, Qatar University, Research Development and Innovation Authority (Saudi Arabia), and US Air Force Office of Scientific Research.

Amine Bermak, holds a master's and Ph.D. in Electrical and Electronic Engineering from Paul Sabatier University, France. He has held various positions in academia and industry in France, the U.K., Australia, Hong Kong, and is currently a Professor and the Associate Dean at Hamad Bin Khalifa University, Qatar. Prof. Bermak has published over 500 articles, designed 50+ chips, and supervised numerous Ph.D. and M.Phil. students. He has received various prestigious awards for his teaching excellence, including the University Michael G. Gale Medal and the Engineering Teaching Excellence Awards at HKUST. He is also an IEEE Distinguished Lecturer.

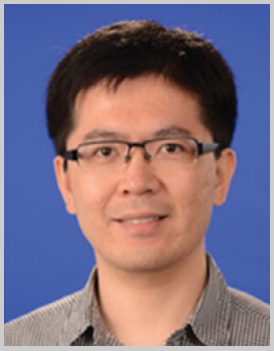

Wen-Di Li is currently an associate professor at the Department of Mechanical Engineering, the University of Hong Kong. He holds a Ph.D. in electrical engineering from Princeton University and Bachelor's and Master's degrees from Tsinghua University. Before joining HKU, he worked on helium ion beam lithography and nanoimprint as a post-doctoral researcher at Hewlett-Packard Labs in California, USA. His research interests mainly focus on high-resolution and scalable lithographic patterning and micro/nanofabrication techniques. Research outcomes from his team have received multiple awards at international conferences and invention exhibitions.

Kabir H Biswas is an Associate Professor in the College of Health & Life Sciences (CHLS), Hamad Bin Khalifa University. He earned his Master's and PhD through the Integrated PhD program at the Indian Institute of Science, India and conducted postdoctoral research at the National University of Singapore and Nanyang Technological University. He takes an interdisciplinary approach, integrating computational methods and experimental techniques such as bioluminescence-based biosensors and biointerfaces, to advance fundamental understanding and development of potential treatment for cancer metastasis, cardiovascular diseases, and infectious diseases. He is also working towards developing point-of-care tests for health and disease monitoring.

Bo Wang is an Associate Professor and a founding faculty in the College of Science and Engineering, Hamad Bin Khalifa University (HBKU). He received his Master's and Ph.D. degrees in electronic and computer engineering from The Hong Kong University of Science and Technology (HKUST), Hong Kong. Afterward, he was with the Massachusetts Institute of Technology, MA, USA, on low-power data converter design for graphene-based pressure sensor. His research interests include energy-efficient analog mixed-signal circuits, sensor and sensor interfaces, and aims to develop heterogeneous integrated systems for in vitro/vivo health monitoring.